

I n t e r n a t i o n a l T e l e c o m m u n i c a t i o n U n i o n

ITU-T

TELECOMMUNICATION
STANDARDIZATION SECTOR
OF ITU

G.650.2

(01/2005)

SERIES G: TRANSMISSION SYSTEMS AND MEDIA,
DIGITAL SYSTEMS AND NETWORKS

Transmission media characteristics – Optical fibre cables

**Definitions and test methods for statistical and
non-linear related attributes of single-mode fibre
and cable**

ITU-T Recommendation G.650.2



ITU-T G-SERIES RECOMMENDATIONS
TRANSMISSION SYSTEMS AND MEDIA, DIGITAL SYSTEMS AND NETWORKS

INTERNATIONAL TELEPHONE CONNECTIONS AND CIRCUITS	G.100–G.199
GENERAL CHARACTERISTICS COMMON TO ALL ANALOGUE CARRIER-TRANSMISSION SYSTEMS	G.200–G.299
INDIVIDUAL CHARACTERISTICS OF INTERNATIONAL CARRIER TELEPHONE SYSTEMS ON METALLIC LINES	G.300–G.399
GENERAL CHARACTERISTICS OF INTERNATIONAL CARRIER TELEPHONE SYSTEMS ON RADIO-RELAY OR SATELLITE LINKS AND INTERCONNECTION WITH METALLIC LINES	G.400–G.449
COORDINATION OF RADIOTELEPHONY AND LINE TELEPHONY	G.450–G.499
TRANSMISSION MEDIA CHARACTERISTICS	G.600–G.699
General	G.600–G.609
Symmetric cable pairs	G.610–G.619
Land coaxial cable pairs	G.620–G.629
Submarine cables	G.630–G.649
Optical fibre cables	G.650–G.659
Characteristics of optical components and subsystems	G.660–G.699
DIGITAL TERMINAL EQUIPMENTS	G.700–G.799
DIGITAL NETWORKS	G.800–G.899
DIGITAL SECTIONS AND DIGITAL LINE SYSTEM	G.900–G.999
QUALITY OF SERVICE AND PERFORMANCE – GENERIC AND USER-RELATED ASPECTS	G.1000–G.1999
TRANSMISSION MEDIA CHARACTERISTICS	G.6000–G.6999
DATA OVER TRANSPORT – GENERIC ASPECTS	G.7000–G.7999
ETHERNET OVER TRANSPORT ASPECTS	G.8000–G.8999
ACCESS NETWORKS	G.9000–G.9999

For further details, please refer to the list of ITU-T Recommendations.

ITU-T Recommendation G.650.2

Definitions and test methods for statistical and non-linear related attributes of single-mode fibre and cable

Summary

This Recommendation contains definitions of the statistical and non-linear parameters of single-mode fibre and cable. It also contains both Reference Test Methods and Alternative Test Methods for characterizing these parameters.

Source

ITU-T Recommendation G.650.2 was approved on 13 January 2005 by ITU-T Study Group 15 (2005-2008) under the ITU-T Recommendation A.8 procedure.

History

Version		Approval
1.0	G.650	1993-03-12
2.0	G.650	1997-04-08
3.0	G.650	2000-10-06
4.0	G.650.2	2002-06-29
4.1	G.650.2 (2002) Amd.1	2003-03-16
5.0	G.650.2	2005-01-13

FOREWORD

The International Telecommunication Union (ITU) is the United Nations specialized agency in the field of telecommunications. The ITU Telecommunication Standardization Sector (ITU-T) is a permanent organ of ITU. ITU-T is responsible for studying technical, operating and tariff questions and issuing Recommendations on them with a view to standardizing telecommunications on a worldwide basis.

The World Telecommunication Standardization Assembly (WTSA), which meets every four years, establishes the topics for study by the ITU-T study groups which, in turn, produce Recommendations on these topics.

The approval of ITU-T Recommendations is covered by the procedure laid down in WTSA Resolution 1.

In some areas of information technology which fall within ITU-T's purview, the necessary standards are prepared on a collaborative basis with ISO and IEC.

NOTE

In this Recommendation, the expression "Administration" is used for conciseness to indicate both a telecommunication administration and a recognized operating agency.

Compliance with this Recommendation is voluntary. However, the Recommendation may contain certain mandatory provisions (to ensure e.g. interoperability or applicability) and compliance with the Recommendation is achieved when all of these mandatory provisions are met. The words "shall" or some other obligatory language such as "must" and the negative equivalents are used to express requirements. The use of such words does not suggest that compliance with the Recommendation is required of any party.

INTELLECTUAL PROPERTY RIGHTS

ITU draws attention to the possibility that the practice or implementation of this Recommendation may involve the use of a claimed Intellectual Property Right. ITU takes no position concerning the evidence, validity or applicability of claimed Intellectual Property Rights, whether asserted by ITU members or others outside of the Recommendation development process.

As of the date of approval of this Recommendation, ITU [had/had not] received notice of intellectual property, protected by patents, which may be required to implement this Recommendation. However, implementors are cautioned that this may not represent the latest information and are therefore strongly urged to consult the TSB patent database.

© ITU 2005

All rights reserved. No part of this publication may be reproduced, by any means whatsoever, without the prior written permission of ITU.

CONTENTS

	Page
1 Scope	1
2 References.....	1
2.1 Normative references.....	1
2.2 Informative references.....	1
3 Terms and definitions	2
3.1 polarization mode dispersion (PMD)	2
3.2 Types of test methods.....	6
4 Abbreviations and acronyms	7
5 Test methods.....	7
5.1 Test methods for polarization mode dispersion.....	7
5.2 Test methods for non-linear attributes.....	37
Appendix I – Determination of PMD delay from an interferogram	37
I.1 RMS calculation for TINTY	37
I.2 RMS calculation for GINTY	39
Appendix II – Non-linear attributes	40
II.1 Background.....	40
II.2 Effective area (A_{eff})	40
II.3 Correction factor k.....	41
II.4 Non-linear coefficient (n^2/A_{eff})	44
II.5 Stimulated Brillouin scattering.....	44
II.6 Other effects	48
Appendix III – Test methods for effective area (A_{eff}).....	48
III.1 The far-field scan (FFS) technique.....	48
III.2 The variable aperture (VA) technique	51
III.3 The near-field scan (NFS) technique.....	54
Appendix IV – Information on polarization mode dispersion statistics	56
IV.1 Introduction	56
IV.2 Data collection.....	57
IV.3 Calculation of PMD_Q (Monte Carlo).....	57
IV.4 Calculation for DGD_{max} (Monte Carlo).....	58

ITU-T Recommendation G.650.2

Definitions and test methods for statistical and non-linear related attributes of single-mode fibre and cable

1 Scope

This Recommendation contains definitions and test methods suitable mainly for factory measurements of the statistical and non-linear attributes of the single-mode optical fibres and cables described in ITU-T Recs G.652, G.653, G.654 and G.655. These definitions and test methods are generally not appropriate for multimode fibre, such as that described in ITU-T Rec. G.651. Some of the test methods, when so indicated, may also be used to characterize discrete optical components, such as those described in ITU-T Rec. G.671. ITU-T Rec. G.650.1 contains definitions and test methods for linear deterministic attributes.

2 References

2.1 Normative references

The following ITU-T Recommendations and other references contain provisions which, through reference in this text, constitute provisions of this Recommendation. At the time of publication, the editions indicated were valid. All Recommendations and other references are subject to revision; users of this Recommendation are therefore encouraged to investigate the possibility of applying the most recent edition of the Recommendations and other references listed below. A list of the currently valid ITU-T Recommendations is regularly published. The reference to a document within this Recommendation does not give it, as a stand-alone document, the status of a Recommendation.

– None.

2.2 Informative references

- [1] ITU-T Recommendation G.652 (2005), *Characteristics of a single-mode optical fibre cable*.
- [2] ITU-T Recommendation G.653 (2003), *Characteristics of a dispersion-shifted single-mode optical fibre cable*.
- [3] ITU-T Recommendation G.654 (2004), *Characteristics of a cut-off shifted single-mode optical fibre and cable*.
- [4] ITU-T Recommendation G.655 (2003), *Characteristics of a non-zero dispersion-shifted single-mode optical fibre and cable*.
- [5] ITU-T Recommendation G.650.1 (2004), *Definitions and test methods for linear, deterministic attributes of single-mode fibre and cable*.
- [6] ITU-T Recommendation G.671 (2005), *Transmission characteristics of optical components and subsystems*.
- [7] ITU-T Recommendation G.663 (2000), *Application related aspects of optical amplifier devices and subsystems*.

3 Terms and definitions

This Recommendation defines the following terms:

3.1 polarization mode dispersion (PMD)

3.1.1 the phenomenon of PMD: Polarization mode dispersion is the differential group delay (DGD) time between two orthogonal polarized modes, which causes pulse spreading in digital systems and distortions in analogue systems.

NOTE 1 – In ideal circular symmetric fibres, the two polarization modes propagate with the same velocity. However, real fibres cannot be perfectly circular and can undergo local stresses; consequently, the propagating light is split into two local polarization modes travelling at different velocities. These asymmetry characteristics vary randomly along the fibre and in time, leading to a statistical behaviour of PMD. A "maximum" value of DGD can be inferred from the statistics.

NOTE 2 – For a given arbitrarily deployed fibre at a given time and optical frequency, there always exist two polarization states, called principal states of polarization ((PSP), see 3.1.2) such that the pulse spreading due to PMD vanishes, if only one PSP is excited. On the contrary, the maximum pulse spread due to PMD occurs when both PSPs are equally excited, and is related to the difference in the group delays associated with the two PSPs.

3.1.2 principal states of polarization (PSP): When operating an optical fibre at a wavelength longer than the cut-off wavelength in a quasi-monochromatic regime, the output PSPs are the two orthogonal output states of polarization for which the output polarizations do not vary when the optical frequency is varied slightly. The corresponding orthogonal input polarization states are the input PSPs.

NOTE 1 – The local birefringence changes along the fibre, and the PSP depends on the fibre length (contrary to hi-bi fibres).

NOTE 2 – The PSPs are random complex vectors depending on time and optical frequency. However, according to the definition, there exists a small frequency range, the PSP bandwidth, over which they can be considered practically constant.

NOTE 3 – If a signal has a bandwidth broader than the PSPs bandwidth, second order PMD effects come into play. They may imply a depolarization of the output field, together with an additional chromatic dispersion effect.

3.1.3 differential group delay ($[\delta\tau(v)]$ in ps): The Differential Group Delay (DGD) is the time difference in the group delays of the PSPs.

The DGD between two PSPs is wavelength dependent and can vary randomly in time due to random mode coupling and randomized stresses along the optical propagation path due, among other causes, to environmental conditions. Variations in the order of a factor of two are typical for normal transmission fibres. As the PMD increases, the variance of the DGD values increases and the characteristic periodicity also decreases. For normal random-mode coupled fibre, the DGD distribution is ergodic, which means that the distribution remains the same over time and wavelength, for a sufficiently long period or wide range. This allows an assumption that measurements over a finite wavelength range are representative of other wavelength ranges or the same wavelength range at different times over a long period of time. For mode coupled fibres, the distribution is normally Maxwellian.

Instantaneous DGD values limit the transmission capacity of digital systems. The derivative of the DGD with respect to the wavelength limits the signal-to-noise ratio (SNR) in analogue systems. Therefore, the statistical distribution of the DGDs (vs time and/or vs wavelength) plays an important role in predicting real system performance.

Negligible mode coupling is found on some specialty fibre such as polarization maintaining fibres (PMF) and some components. For these devices there is very little DGD variation with wavelength.

3.1.4 PMD value: PMD_{AVG} defined as the linear average $\langle \Delta\tau \rangle$ of the DGD values $\Delta\tau(\nu)$ over a given optical frequency range ν_1 to ν_2 ,

$$PMD_{AVG} = \langle \Delta\tau \rangle = \frac{\int_{\nu_1}^{\nu_2} \Delta\tau(\nu) d\nu}{\nu_2 - \nu_1} \quad (3-1)$$

PMD_{RMS} defined as the root-mean square (RMS) $\langle \Delta\tau^2 \rangle^{1/2}$ of the DGD values $\Delta\tau(\nu)$ over a given optical frequency range ν_1 to ν_2 ,

$$PMD_{RMS} = \langle \Delta\tau^2 \rangle^{1/2} = \left(\frac{\int_{\nu_1}^{\nu_2} \Delta\tau(\nu)^2 d\nu}{\nu_2 - \nu_1} \right)^{1/2} \quad (3-2)$$

NOTE 1 – For Equations 3-1 and 3-2 to be valid, the range ν_1 to ν_2 should be sufficiently wide, such as for instance of the order of 100 nm in corresponding wavelength range.

If the distribution of these DGD values over the given optical frequency range may be approximated by a Maxwell distribution with sufficient amount of confidence and fidelity, PMD_{avg} can be mathematically related to PMD_{RMS} .

$$\langle \Delta\tau \rangle = \left(\frac{8}{3\pi} \right)^{1/2} \langle \Delta\tau^2 \rangle^{1/2} \quad (3-3)$$

For fibre and cable, the PMD Reference Test Method (RTM) reports the linear average.

NOTE 2 – Averaging over temperature, time or mechanical perturbations is generally an acceptable alternative to averaging over frequency. In this case, the expected value operator is over all conditions. The expected value of a set of finite wavelengths at a given time is equal to the long term expected value over any frequency range. Both Equations 3-1 and 3-2 are considered as an averaging in this context.

NOTE 3 – Equation 3-3 applies only when the distribution of DGDs is Maxwellian, for instance, when the fibre is randomly mode coupled. The generalized use of Equation 3-3 can be verified by statistical analysis. A Maxwell distribution may not be the case if there are point sources of elevated birefringence (relative to the rest of the fibre), such as a tight bend, or other phenomena that reduce the mode coupling, such as a continual reduced bend radius with fibre in tension. In these cases, the distribution of the DGDs will begin to resemble the square root of a non-central Chi-square distribution with three degrees of freedom. For these cases, the PMD_{RMS} value will generally be larger relative to the PMD_{AVG} that is indicated in Equation 3-3. Time domain methods such as Method C and Method A, cosine Fourier transform, which are based on PMD_{RMS} , can use Equation 3 to convert to PMD_{AVG} . If mode coupling is reduced, the resultant reported PMD value from these methods may exceed those that can be reported by the frequency domain measurements that report PMD_{AVG} , such as Method B.

3.1.5 PMD coefficient: The PMD value normalized to the measurement length:

There are two normalization formulas, one for random mode coupling, associated with normal transmission fibres, and one for negligible mode coupling, associated with specialty fibres such as polarization maintaining fibres.

For random mode coupling, the PMD coefficient is the PMD value (PMD_{avg} or PMD_{RMS}) divided by the square root of the length ($L^{1/2}$) and is usually reported in units of ps/km^{1/2}.

For negligible mode coupling, the PMD coefficient is the PMD value (PMD_{avg} or PMD_{RMS}) divided by the length (L) and may be reported in units of ps/km or fs/m.

3.1.6 Mathematical definitions

PMD can be described in terms of Stokes or Jones vectors. The evolution of the output Jones vector with angular optical frequency, $\omega = 2\pi\nu = 2\pi c/\lambda$, is the source of system impairment. The following is based on the assumption of negligible polarization dependent loss (PDL).

The relationship of the Stokes vector, \hat{s} , and the associated Jones vector, \hat{j} , is:

$$\hat{s} = \begin{bmatrix} \cos 2\theta \\ \sin 2\theta \cos \mu \\ \sin 2\theta \sin \mu \end{bmatrix} \Leftrightarrow \hat{j} = \begin{bmatrix} \cos \theta \exp(-i\mu/2) \\ \sin \theta \exp(i\mu/2) \end{bmatrix} \quad (3-4)$$

where:

θ is the linear SOP angle (half the rotation angle on the equator of the Poincaré sphere.

μ is the elevation angle from the equator of the Poincaré sphere and also the phase difference between the elements of the Jones vector.

For a given frequency, ω_0 , the relationship between the input Stokes vector, \hat{s}_0 , to output vector can be described as a rotation, R , with rotation angle, γ_{ROT} , and rotation vector, \hat{y} .

$$\hat{s} = R\hat{s}_0 \quad \text{where} \quad R = \hat{y}\hat{y}^T(1 - \cos \gamma_{ROT}) + I \cos \gamma_{ROT} + [\hat{y} \times] \sin \gamma_{ROT} \quad (3-5)$$

$[\hat{y} \times]$ is the cross product operator and I is the identity matrix.

At this frequency, the relationship of the output Jones vector to input vector, \hat{j}_0 , is given by the matrix, T , as:

$$\hat{j} = T\hat{j}_0 \quad \text{where} \quad T = \begin{bmatrix} \cos \gamma_T - iy_1 \sin \gamma_T & -\sin \gamma_T (y_3 + iy_2) \\ \sin \gamma_T (y_3 - iy_2) & \cos \gamma_T + iy_1 \sin \gamma_T \end{bmatrix} \quad (3-6)$$

$\gamma_{ROT} = 2\gamma_T$ and the subscripted values are the elements of the rotation vector

The polarization dispersion vector (PDV), $\hat{\Omega}$, is used to describe the variation of the output vectors with frequency. In the Stokes notation, it is defined as:

$$\left. \frac{d\hat{s}(\omega)}{d\omega} \right|_{\omega_0} = \left. \frac{dR(\omega)}{d\omega} \right|_{\omega_0} R^T(\omega_0) \hat{s}(\omega_0) = \hat{\Omega} \times \hat{s}(\omega_0) \quad (3-7a)$$

In the Jones notation, it is defined as follows, where the subscripted values are the elements of the PDV:

$$\left. \frac{d\hat{j}(\omega)}{d\omega} \right|_{\omega_0} = \left. \frac{dT(\omega)}{d\omega} \right|_{\omega_0} T \times (\omega_0) \hat{j}(\omega_0) = -\frac{i}{2} \begin{bmatrix} \Omega_1 & \Omega_2 - i\Omega_3 \\ \Omega_2 + i\Omega_3 & -\Omega_1 \end{bmatrix} \hat{j}(\omega_0) \quad (3-7b)$$

Equation (3-7b) can be used as the basis of a first order Taylor expansion for the evolution of the output Jones vector in the neighbourhood of ω_0 .

The PDV can be related to the PSP, \hat{p} , and DGD, $\Delta\tau$, as well as the rotation vector and angle as:

$$\hat{\Omega} = 2 \frac{d\gamma_T}{d\omega} \hat{y} + \sin 2\gamma_T \frac{d\hat{y}}{d\omega} + 2 \sin^2 \gamma_T \left(\hat{y} \times \frac{d\hat{y}}{d\omega} \right) = \Delta\tau \hat{p} \quad (3-8)$$

Equation 3-7b can be written as:

$$\left. \frac{d\hat{j}(\omega)}{d\omega} \right|_{\omega_0} = \left. \frac{dT(\omega)}{d\omega} \right|_{\omega_0} T \times (\omega_0) \hat{j}(\omega_0) = -\frac{i}{2} \Delta\tau V_p \begin{bmatrix} 1 & 0 \\ 0 & -1 \end{bmatrix} V_p \times \hat{j}(\omega_0) \quad (3-9)$$

where:

$$V_p = \begin{bmatrix} \cos \theta_p \exp(-i\mu_p/2) & -\sin \theta_p \exp(-i\mu_p/2) \\ \sin \theta_p \exp(i\mu_p/2) & \cos \theta_p \exp(i\mu_p/2) \end{bmatrix}$$

V_p^* is the transpose conjugate of V_p

$$\text{and the PSP is } \hat{p} = \begin{bmatrix} \cos 2\theta_p \\ \sin 2\theta_p \cos \mu_p \\ \sin 2\theta_p \sin \mu_p \end{bmatrix}$$

Assuming that the PSPs are frequency invariant (over a narrow frequency interval, ω_0 and $\omega_0 + \Delta\omega$), Equation 3-7b has a solution in the neighbourhood of ω_0 :

$$\hat{j}(\omega) = V_p \begin{bmatrix} \exp[-i\omega\Delta\tau/2] & 0 \\ 0 & \exp[i\omega\Delta\tau/2] \end{bmatrix} V_p \times \hat{j}(\omega_0) = J(\omega) \hat{j}(\omega_0) \quad (3-10)$$

where ω is deviation from ω_0

In the Stokes notation, Equation 3-10 corresponds to a rotation of $\omega\Delta\tau$ about the PSP on the Poincaré sphere.

Equation 3-10 is written as a singular value decomposition. The diagonal elements of the central matrix are the eigenvalues. The columns of the matrix, V_p , are the eigenvectors, which are in the Jones vector form. The first column converts to the PSP in the same form as in Equation 3-4. Call this \hat{j}_p . This matrix can also be expressed in the form of Equation 3-6, with $\omega\Delta\tau/2$ replacing γ_T and with the elements of the PSP replacing the elements of the rotation vector.

A change of coordinates can be applied to Equation 3-10 so the PSP matrix in the new coordinate system is the identity matrix. The x and y elements of the result can be convolved with the frequency domain field of a monochromatic source which can then be expressed in the time domain as a power function. For example, a Gaussian temporal pulse with RMS width equal to σ (ps) and a fibre with chromatic dispersion, D (ps/nm). The resultant output power function is a split pulse, $P(t)$:

$$P(t) = \frac{1}{S\sqrt{2\pi}} \left\{ \exp\left[-\frac{(t - (\tau_G - \Delta\tau/2))^2}{2S^2}\right] u + \exp\left[-\frac{(t - (\tau_G + \Delta\tau/2))^2}{2S^2}\right] (1-u) \right\} \quad (3-11)$$

where τ_G is the group delay for $u = 0.5$

$$S^2 = \sigma^2 + \left(\frac{\tau'}{2\sigma}\right)^2 \text{ and } \tau' = -D \frac{\lambda_0}{\omega_0}$$

$$u = (\hat{j}_p \times T(\omega_0) \hat{j}_0) \times (\hat{j}_p \times T(\omega_0) \hat{j}_0) \text{ in the original coordinates.}$$

The difference between pulse centre for $u = 0$ is $\Delta\tau$ away from the pulse centre for $u = 1$. This is the meaning of DGD. These values of u are achieved when the output Jones vector is aligned with \hat{j}_p or its orthogonal counterpart, the other eigenvector.

The RMS width of this pulse is:

$$RMS_p = [S^2 + \Delta\tau^2 u(1-u)]^{1/2} \quad (3-12)$$

In measurements using the RTM JME analysis, estimates of the T matrix are calculated for ω_0 and $\omega_0 + \Delta\omega$, a frequency slightly larger. The frequency transfer matrix is approximated as:

$$J(\Delta\omega) = T(\omega_0 + \Delta\omega)T^{-1}(\omega_0) \quad (3-13)$$

It is clear from Equation 3-10 that the argument of the ratio of eigenvalues, divided by $\Delta\omega$, is the DGD.

The term "first-order" was originally associated with the first-order Taylor expansion associated with Equation 3-7b. It could also be associated with the fact that it provides a continuous phase-linear map from the Jones vector at one frequency to the next higher frequency.

Second order PMD could be thought of as a description of $J(\omega)$ that provides a continuous mapping to both the frequency above and the frequency below. This can be done by replacing $\omega\Delta\tau/2$ by a more general expression, $\gamma(\omega)$, that is described as a Taylor expansion:

$$\gamma(\omega) = \omega\gamma_\omega + \omega^2\gamma'_\omega / 2 \quad (3-14a)$$

Similarly, the angular parameters of the PSP can be written as:

$$\theta_p(\omega) = \theta_{p0} + \omega\theta_{p\omega} \quad \text{and} \quad \mu_p(\omega) = \mu_{p0} + \omega\mu_{p\omega} \quad (3-14b)$$

The use of formulae such as Equation 3-13 for the reverse frequency, the singular value decomposition of Equation 3-10, and some algebra/trigonometry can yield estimates of the parameters of Equations 3-14a and 3-14b from measured data.

The second order PDV, $\bar{\Omega}_\omega$, is defined as the frequency derivative of the PDV:

$$\bar{\Omega}_\omega = \frac{d\bar{\Omega}}{d\omega} = \frac{d\Delta\tau}{d\omega} \hat{p} + \Delta\tau \frac{d\hat{p}}{d\omega} \quad (3-15)$$

When random mode coupling is present, the magnitude of this vector and its expected value are related to the PMD value as:

$$\langle \bar{\Omega}_\omega \cdot \bar{\Omega}_\omega \rangle = \left\langle \left(\frac{d\Delta\tau}{d\omega} \right)^2 \right\rangle + \left\langle \Delta\tau^2 \frac{d\hat{p}}{d\omega} \cdot \frac{d\hat{p}}{d\omega} \right\rangle = \frac{1}{3} \langle \Delta\tau^2 \rangle^2 \quad (3-16)$$

The ratio of first term, involving the derivative of the DGD, to the second term, involving the derivative of the PSP, is 1/8. The first term is interactive with chromatic dispersion and the second term has a depolarizing effect.

The convolution of the expanded representation of the frequency transfer matrix with the input pulse is beyond the scope of this clause, but it is clear that the results will not be as easy to represent and will depend on the details of the parameters at the frequency of the source. If, however, one is interested in the expected values, Equation 3-16 makes it clear that these values can be calculated from the PMD_{RMS} value and those explicit measurements are not needed.

3.2 Types of test methods

3.2.1 reference test method (RTM): A test method in which a characteristic of a specified class of optical fibres or optical fibre cables is measured strictly according to the definition of this characteristic and which gives results which are accurate, reproducible and relatable to practical use.

3.2.2 alternative test method (ATM): A test method in which a given characteristic of a specified class of optical fibres or optical fibre cables is measured in a manner consistent with the definition of this characteristic and gives results which are reproducible and relatable to the reference test method and to practical use.

4 Abbreviations and acronyms

This Recommendation uses the following abbreviations:

ATM	Alternative Test Method
DGD	Differential Group Delay
DWDM	Dense Wavelength Division Multiplexing
ECL	External Cavity Laser
FWHM	Full Width at Half Maximum
LD	Laser Diode
LED	Light Emitting Diode
MFD	Mode Field Diameter
NFP	Near-Field Pattern
OTDR	Optical Time Domain Reflectometer
PMD	Polarization Mode Dispersion
PS	Poincaré Sphere
PSP	Principal State of Polarization
RTM	Reference Test Method
SOP	State of Polarization
TBD	To Be Determined
WDM	Wavelength Division Multiplexing

5 Test methods

Both Reference Test Method (RTM) and Alternative Test Methods (ATMs) are usually given here for each parameter and it is the intention that both the RTM and the ATM(s) may be suitable for normal product acceptance purposes. However, when using an ATM, should any discrepancy arise it is recommended that the RTM be employed as the technique for providing the definitive measurement results.

NOTE – The apparatus and procedure given cover only the essential basic features of the test methods. It is assumed that the detailed instrumentation will incorporate all necessary measures to ensure stability, noise elimination, signal-to-noise ratio, etc.

5.1 Test methods for polarization mode dispersion

All the test methods report the PMD value. The conversion to PMD coefficient shall be done according to the definition in 3.1.5.

5.1.1 Reference test method: The Stokes parameter evaluation technique

5.1.1.1 General

This test method describes a procedure for measuring the polarization mode dispersion (PMD) of single-mode optical fibres. The change in the output state of polarization (SOP) with wavelength is determined. This change can be characterized through Jones Matrix Eigenanalysis (JME), or the rotation of the SOP vector on the Poincare Sphere (PS). It can be applied to both short and long fibres, regardless of the degree of polarization mode coupling. Under some circumstances, repeated measurements may be necessary to achieve satisfactory precision. This method is restricted to wavelengths greater than or equal to that at which the fibre is effectively single-mode.

When measuring fibres in motion (e.g., fibres in OPGW), the Interferometer Method could be a better choice for the dispute resolution function of the RTM.

5.1.1.2 Test apparatus

See Figure 1 for a schematic diagram of the key components in a typical measurement system.

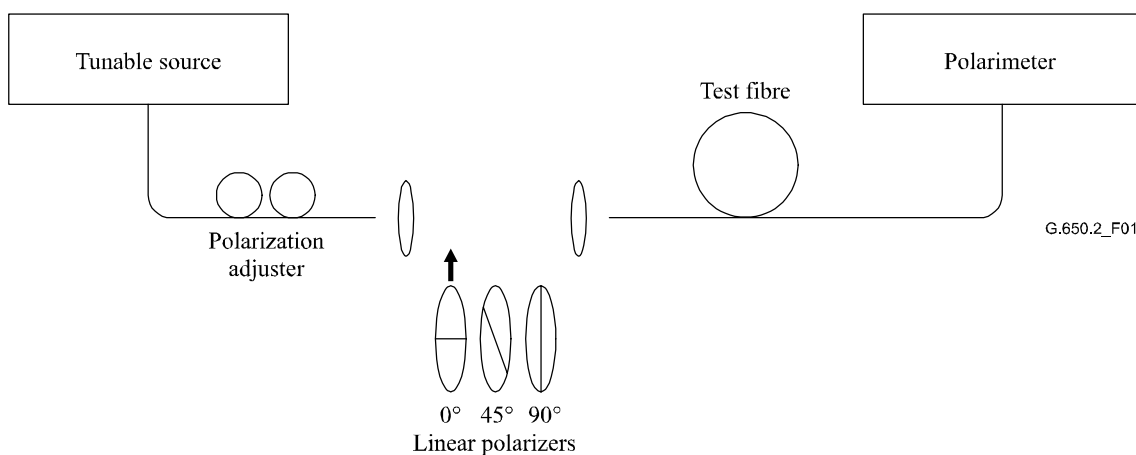


Figure 1/G.650.2 – Schematic diagram of equipment (typical)

5.1.1.2.1 Light source

Use a single-line laser or narrow-band source which is tuneable across the intended measurement wavelength range. The spectral distribution shall be narrow enough so that the light emerging from the test fibre remains polarized under all conditions of the measurement. Degree of Polarization (DOP) of 90% or greater is preferred, although measurements may be performed with values as low as 25% with reduced precision. For a given value of differential group delay $\Delta\tau$, the lowest degree of polarization which can result is given by:

$$DOP = 100e^{-\frac{1}{4 \ln 2} \left(\frac{\pi c \Delta\tau \Delta\lambda_{FWHM}}{\lambda_0^2} \right)^2} \quad (5-1)$$

assuming a Gaussian spectrum of width $\Delta\lambda_{FWHM}$ centered at λ_0 . DOP is expressed as a percentage.

5.1.1.2.2 Polarization adjuster

A polarization adjuster follows the laser and is set to provide roughly circularly polarized light to the polarizers, so that the polarizers never cross polarization with their input light. Adjust polarization as follows. Set the tunable laser wavelength to the centre of the range to be measured. Insert each of the three polarizers into the beam and perform three corresponding power measurements at the output of the polarizers. Adjust the source polarization via the polarization adjuster such that the three powers fall within approximately a 3 dB range of one another. In an

open beam version of the set-up, a waveplate may perform the polarization adjustment.

5.1.1.2.3 Polarizers

Three linear polarizers at relative angles of approximately 45 degrees are arranged to be inserted into the light beam in turn. The actual relative angles shall be known.

5.1.1.2.4 Input optics

An optical lens system or single-mode fibre pigtail may be employed to excite the test fibre.

5.1.1.2.5 Fibre pigtail

If pigtails are used, interference effects due to reflections should be avoided. This may require index matching materials or angled cleaves. The pigtails shall be single-mode.

5.1.1.2.6 Optical lens system

If an optical lens system is used, some suitable means, such as a vacuum chuck, shall be used to stably support the input end of the fibre.

5.1.1.2.7 Cladding mode stripper

Remove any cladding mode power from the test fibre. Under most circumstances, the fibre coating will perform this function; otherwise, employ a device that extracts cladding mode power.

5.1.1.2.8 Output optics

Couple all power emitted from the test fibre to the polarimeter. An optical lens system, a butt splice to a single-mode fibre pigtail or an index-matched coupling made directly to the detector system are examples of means that may be used.

5.1.1.2.9 Polarimeter

Use a polarimeter to measure the three output states of polarization corresponding to insertion of each of the three polarizers. The wavelength range of the polarimeter shall include the wavelengths produced by the light source.

5.1.1.3 Measurement procedure

The test sample shall be a known length of a single-mode optical fibre which may or may not be cabled. The sample and pigtails shall be fixed in position at a nominally constant temperature throughout the measurement. Temperature stability of the test device may be observed by viewing the output state of polarization of the test fibre on a Poincaré sphere display. In a time period corresponding to an adjacent pair of Jones matrix measurements, output polarization change should be small relative to the change produced by a wavelength increment.

NOTE – Although the test sample is normally a fibre, this test can also be performed on discrete components. In this case, PMD coefficient is not relevant.

It is important to minimize deployment-induced mode coupling when measuring uncabled fibres, which is done in order to support the primary requirements of cabled fibre PMD_Q . In this case, the fibre shall be supported in some manner (usually on a reel having a minimum wind radius of 150 mm), with essentially zero fibre tension (typically less than 5 g), and no tensioned crossovers. These deployment requirements can limit the length that can be measured, depending on the spool diameter, and can make the measurement a destructive one. Multi-layer windings are possible, but should be qualified by comparison with single-layer results on shorter lengths.

The measurement of uncabled fibre deployed on shipping spools is not recommended. PMD results with this deployment have been shown to be substantially less than what would be obtained in cable form for high PMD fibre and substantially greater than what would be obtained in cable form for low PMD fibre.

Couple the light source through the polarization adjuster to the polarizers.

Couple the output of the polarizers to the input of the fibre under test.

Couple the output of the fibre under test to the input of the polarimeter.

Select the wavelength interval $\Delta\lambda$ over which the measurements are to be performed. The maximum allowable value of $\Delta\lambda$ (around λ_0) is set by the requirement:

$$\Delta\tau_{\max}\Delta\lambda \leq \frac{\lambda_0^2}{2c} \quad (5-2)$$

where $\Delta\tau_{\max}$ is the maximum expected DGD within the measurement wavelength range. For example, the product of maximum DGD and wavelength interval shall remain less than 4 ps.nm at 1550 nm and less than 2.8 ps.nm at 1300 nm. This requirement ensures that from one test wavelength to the next, the output state of polarization rotates less than 180 degrees about the principal states axis of the Poincaré sphere. If a rough estimate of $\Delta\tau_{\max}$ cannot be made, perform a series of sample measurements across the wavelength range, each measurement using a closely spaced pair of wavelengths appropriate to the spectral width and minimum tuning step of the optical source. Multiply the maximum DGD measured in this way by a safety factor of three, substitute this value for $\Delta\tau_{\max}$ in the above expression and compute the value of $\Delta\lambda$ to be used in the actual measurement. If there is concern that the wavelength interval used for a measurement was too large, the measurement may be repeated with a smaller wavelength interval. If the shape of the curve of DGD vs. wavelength and the mean DGD are essentially unchanged, the original wavelength interval was satisfactory.

Gather the measurement data. At the selected wavelengths, insert each of the polarizers and record corresponding Stokes parameters from the polarimeter.

5.1.1.4 Calculations or interpretation of result

There are two ways (JME and PSA) of analysing the Stokes parameters that were measured in 5.1.1.3. Both analysis methods deduce the rotation of the output Stokes vectors at one optical frequency to the next frequency. The DGD is proportional to the rotation angle and inversely proportional to the frequency difference. The two methods are mathematically equivalent for first-order PMD for negligible PDL.

The Stokes parameters for a given wavelength are the normalized Stokes output vectors which are represented as \hat{H} , \hat{Q} , and \hat{V} for relative input linear SOP angles of 0° , 45° , and 90° respectively.

In clause 5.1.3, wavelength was used to describe the measurement. Angular optical frequency, $\omega = 2\pi c/\lambda$ (ps^{-1}) is the most useful metric for the calculations. The calculations below are given for a single pair of adjacent frequencies designated as ω_0 and $\omega_0 + \Delta\omega$. This pair yields a DGD value. The DGD values are calculated for each ascending pair of frequencies over a frequency range using the same calculations.

The average of all the DGD values is reported as the PMD value.

5.1.1.4.1 Jones matrix eigen-analysis

For a given frequency, use Equation 3-4 to convert the measured unit output Stokes vectors to Jones vectors by assuming that $0 \leq \theta \leq \pi$. The complex x and y elements of these vectors are designated as: h_x , h_y , q_x , q_y , v_x , and v_y . Using these, calculate the following ratios:

$$k_1 = h_x / h_y, \quad k_2 = v_x / v_y, \quad k_3 = q_x / q_y, \quad k_4 = \frac{k_3 - k_2}{k_1 - k_3} \quad (5-3)$$

The assumption of $0 \leq \theta \leq \pi$ is not relevant because of the ratio calculations.

For the frequency, the Jones transfer matrix, T, is calculated as:

$$T = \begin{bmatrix} k_1 k_4 & k_2 \\ k_4 & 1 \end{bmatrix} \quad (5-4)$$

The actual transfer matrix is the matrix of Equation 5-4 times an unknown complex constant which is inversely proportional to the square root of the determinant of the calculated matrix. This constant is not needed for the rest of the calculations, however.

For a pair of frequencies, the Jones frequency transfer matrix, J, is calculated as:

$$J(\omega_0) = T(\omega_0 + \Delta\omega)T^{-1}(\omega_0) \quad (5-5)$$

Calculate the two Eigen-values, $\rho_1(\omega_0)$ and $\rho_2(\omega_0)$ of J(ω_0). The DGD, $\Delta\tau(\omega_0)$ is given as:

$$\Delta\tau(\omega_0) = \frac{|\arg(\rho_1(\omega_0)/\rho_2(\omega_0))|}{\Delta\omega} \quad (5-6)$$

where

$\arg(me^{i\theta}) = \theta$ with m and θ both real, and $|\theta| < \pi$.

The data may be displayed as a function of wavelength as shown in Figure 2 or as a histogram as in Figure 3.

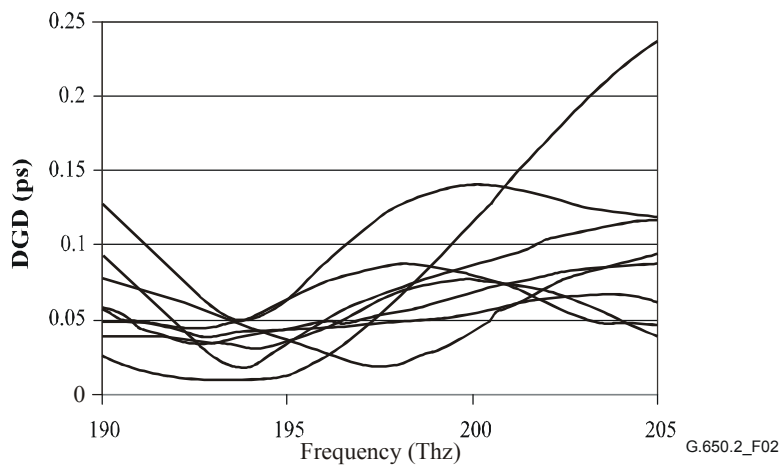


Figure 2/G.650.2 – DGD data vs frequency

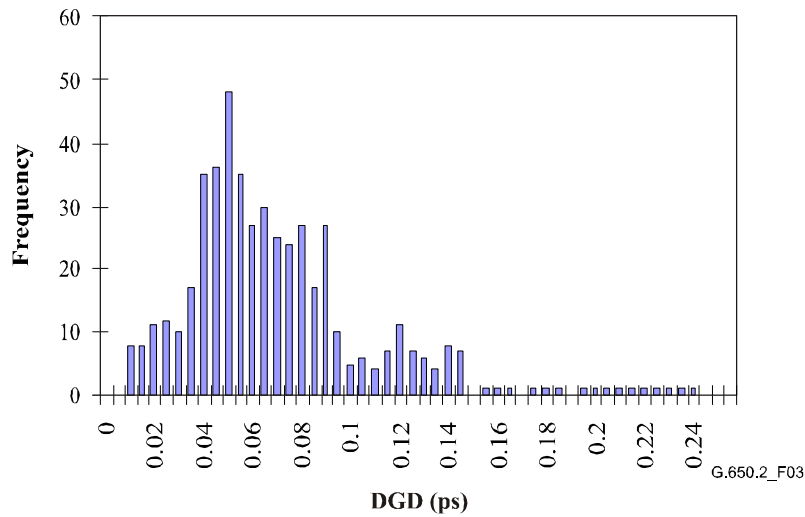


Figure 3/G.650.2 – DGD data as a histogram

5.1.1.4.2 Poincaré sphere analysis (PSA)

The analysis is based on an arcsine function to determine the rotation of the normalized Stokes vectors on the Poincaré sphere.

From the measured normalized Stokes vectors \hat{H} , \hat{V} , \hat{Q} , compute:

$$\hat{h} = \hat{H}, \quad \hat{q} = \frac{\hat{H} \times \hat{Q}}{|\hat{H} \times \hat{Q}|} \times \hat{H}, \quad \hat{v} = \frac{\hat{q} \times \hat{V}}{|\hat{q} \times \hat{V}|} \times \hat{q} \quad (5-7)$$

This makes the analysis independent of the input SOPs and consequently having no need to know them.

From the Stokes vectors \hat{h} , \hat{v} and \hat{q} , form the vector products $\hat{c} = \hat{h} \times \hat{q}$ and $\hat{c}' = \hat{q} \times \hat{v}$ at each wavelength. For each frequency increment, compute the finite differences,

$$\begin{aligned} \Delta \hat{h} &= \hat{h}(\omega_0 + \Delta\omega) - \hat{h}(\omega_0) & \Delta \hat{q} &= \hat{q}(\omega_0 + \Delta\omega) - \hat{q}(\omega_0) & \Delta \hat{v} &= \hat{v}(\omega_0 + \Delta\omega) - \hat{v}(\omega_0) \\ \Delta \hat{c} &= \hat{c}(\omega_0 + \Delta\omega) - \hat{c}(\omega_0) & \Delta \hat{c}' &= \hat{c}'(\omega_0 + \Delta\omega) - \hat{c}'(\omega_0) \end{aligned} \quad (5-8)$$

Find the DGD, $\Delta\tau$, for a particular frequency increment from the following expression:

$$\Delta\tau = \frac{1}{\Delta\omega} \cdot \left[\arcsin\left(\frac{1}{2} \sqrt{\frac{1}{2} (\Delta \hat{h}^2 + \Delta \hat{q}^2 + \Delta \hat{c}^2)}\right) + \arcsin\left(\frac{1}{2} \sqrt{\frac{1}{2} (\Delta \hat{q}^2 + \Delta \hat{v}^2 + \Delta \hat{c}'^2)}\right) \right] \quad (5-9)$$

NOTE – $\Delta \hat{h}^2 = \Delta \hat{h} \cdot \Delta \hat{h}$

5.1.1.5 Presentation of the results

- a) Identification of the sample measured.
- b) Test length.
- c) The wavelength range over which the measurement was performed, the wavelength step size, and the number of sampled points.
- d) The physical configuration of the fibre or cable sample.
- e) Mode coupling type (negligible, semi-random, or random).
- f) Method of analysis (JME or PS).

- g) PMD in ps. If the degree of mode coupling is known, the PMD coefficient may be given in ps/km (negligible mode coupling), or ps/km^{1/2} (random mode coupling).
- h) When an average PMD has been determined from repeated measurements of the sample, record the number of measurements performed.

5.1.2 First alternative test method: State of polarization (SOP) method

5.1.2.1 General

This method measures the trajectory of the output Stokes vector as a function of frequency from a single input SOP. The analysis yields an estimate of the rotation angle from each frequency to the next. A weakness of this method is that if the output Stokes vector comes into alignment with the PSP, the estimated DGD can be significantly less than the actual value.

The method is based on the fact that when the optical frequency of the launched light is varied, the polarization state at the output of the fibre, represented on the Poincaré sphere in the space of the Stokes parameters, rotates around the axis coinciding with the direction of the PSPs at a rate dependent on the PMD delay: the greater the delay, the faster the rotation. Therefore by measuring the rotation angle $\Delta\theta$ of the representative point on the Poincaré sphere corresponding to angular frequency variation $\Delta\omega$ the PMD delay, $\Delta\tau$, is obtained as:

$$\Delta\tau = \left| \frac{\Delta\theta}{\Delta\omega} \right| \quad (5-10)$$

It should be noted that when one of the input PSPs is excited, the corresponding SOP at the fibre output remains unchanged by definition and no rotation is detected on the Poincaré sphere.

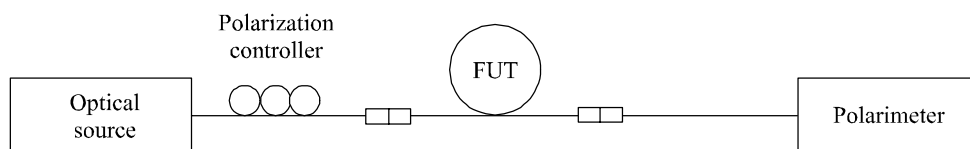
The technique provides directly the Differential Group Delays (DGDs) between the principal states of polarization of the fibre under test as a function of wavelength or time. The PMD is obtained by suitable averaging over time or wavelength or both. The method is able to give complete information about the statistics of the DGDs.

5.1.2.2 Test apparatus

A schematic diagram of the test apparatus is shown in Figure 4. The technique involves measuring the output state of polarization of the fibre under test at a number of wavelengths across a given spectral range by launching in the fibre under test light with a fixed state of polarization.

5.1.2.2.1 Optical source

A stable single-line laser, tunable across the measurement wavelength range, is required. The spectral width of the laser must be narrow enough to ensure that depolarization of the signal, due to the PMD of the fibre under test, does not occur.



G.650.2_F04

Figure 4/G.650.2 – Schematic of the apparatus for PMD measurement by state of polarization analysis

5.1.2.2.2 Polarization controller

A polarization controller shall be placed between the optical source and the fibre under test.

5.1.2.2.3 Polarimeter

A polarimeter to measure the Stokes parameters as a function of wavelength at the output of the fibre under test shall be used.

5.1.2.2.4 Samples

The test sample shall be of known length of single-mode fibre which may or may not be cabled. The sample and pigtails must be fixed in position at a nominally constant temperature throughout the measurement. The standard ambient conditions shall be employed. In the case of installed fibres and cables, prevailing deployment conditions may be used.

It is important to minimize deployment-induced mode coupling when measuring uncabled fibres, which is done in order to support the primary requirements of cabled fibre PMD_Q . In this case, the fibre shall be supported in some manner (usually on a reel having a minimum wind radius of 150 mm), with essentially zero fibre tension (typically less than 5 g), and no tensioned crossovers. These deployment requirements can limit the length that can be measured, depending on the spool diameter, and can make the measurement a destructive one. Multi-layer windings are possible, but should be qualified by comparison with single-layer results on shorter lengths.

The measurement of uncabled fibre deployed on shipping spools is not recommended. PMD results with this deployment have been shown to be substantially less than what would be obtained in cable form for high PMD fibre and substantially greater than what would be obtained in cable form for low PMD fibre.

NOTE – Although the test sample is normally a fibre, this test can also be performed on discrete components. In this case, PMD coefficient is not relevant.

5.1.2.3 Measurement procedure

5.1.2.3.1 Measurement

- a) The light exiting the optical source is passed through the polarization controller and coupled to the fibre under test. The polarization controller is set so as to optimize the conditions for the determination of the rotation angle on the Poincaré sphere, if necessary. If the paths are in fibre, ensure that the fibres are stationary during the measurements to follow.
- b) The output of the fibre under test is coupled to the input of the polarimeter.
- c) Select the wavelength range over which the measurement is to be performed.
- d) Select the wavelength step $\Delta\lambda$ (in nm) at which Stokes parameters are to be measured. To avoid that the output state of polarization (PSP) rotates more than 180° about the PSPs axis on the Poincaré sphere from one test wavelength to the next, the requirement $\Delta\tau_{\max} \Delta\lambda \leq 4$ ps.nm should be fulfilled, where $\Delta\tau_{\max}$ (in ps) is the maximum expected DGD of the fibre under test.
- e) The measured values of the Stokes parameters at the selected wavelengths value are recorded in a way suitable for the analysis described in the following clauses.

5.1.2.3.2 Calculation or interpretation of results

After the polarization fluctuation has been measured by the Stokes analyser (or rotatable analyser), it can be transformed into the SOP curve as a function of wavelength (frequency).

The SOP is expressed as:

$$SOP = \frac{1 - \eta^2}{1 + \eta^2} \quad (5-11)$$

where:

$$\eta = \tan \left[0.5 \tan^{-1} \left\{ S_3 / \sqrt{S_1^2 + S_2^2} \right\} \right] \quad (5-12)$$

Here, η is the polarization ellipticity, S_1 , S_2 and S_3 are Stokes parameters.

In Figure 5, the peak (or extrema) to peak of SOP curves is equivalent to the phase difference of π .

The DGD or PMD $\delta\tau$ is given by:

$$\Delta\tau = \frac{N}{2} \cdot \frac{1}{\Delta f} = \frac{N}{2} \cdot \frac{\lambda_1 \lambda_n}{c \Delta\lambda} \quad (5-13)$$

where N represents the numbers from extrema to extrema of SOP curves.

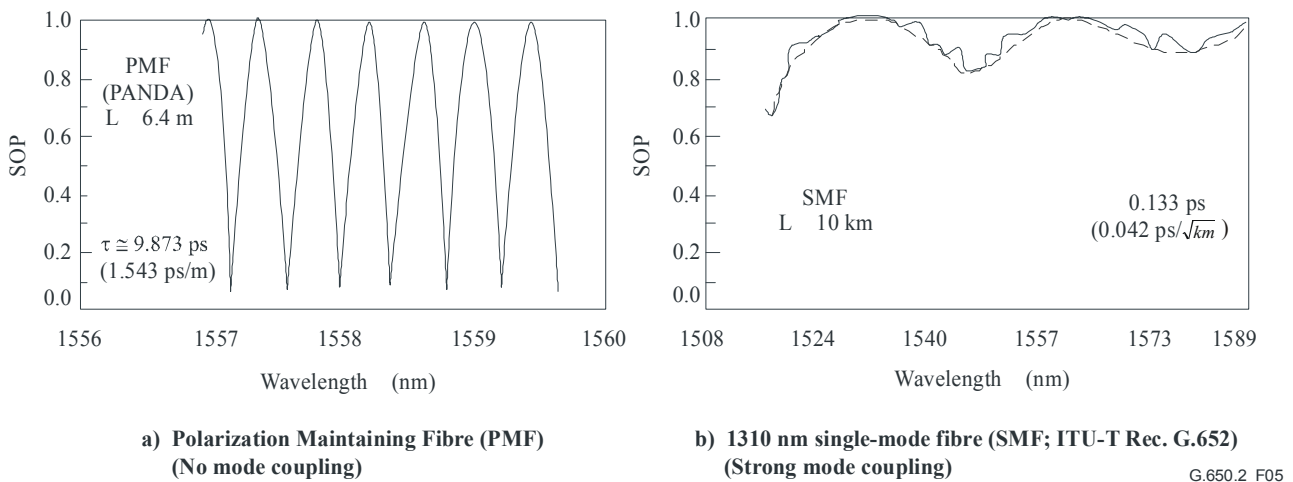


Figure 5/G.650.2 – State of Polarization (SOP) representation of two examples of PMD measurements

5.1.2.4 Presentation of the results

- a) Test set-up arrangement, processing algorithms.
- b) Wavelength range, wavelength step, number of sampled points.
- c) Temperature of the sample and environmental conditions.
- d) Fibre identification and length.
- e) Fibre deployment conditions.
- f) Indication of the accuracy and repeatability.
- g) Plot of the accuracy and repeatability.
- h) Histogram of the measured DGDs versus wavelength (if required).
- i) Mean DGD.
- j) PMD coefficient.

5.1.3 Second alternative test method: Interferometric method

5.1.3.1 General

This test method describes a procedure for measuring the PMD of single-mode optical fibres and cables.

The measured value represents PMD_{RMS} over a broad measurement wavelength range of typical broadband sources such as LED, combination of super LED's or amplified spontaneous emission (ASE) source in the 1310 nm or the 1550 nm window or any other window of interest, depending on the user requirements.

The PMD is determined from an interferogram containing the autocorrelation and cross-correlation function of the emerging electromagnetic field at one end of the fibre under test (FUT) when illuminated by the broadband polarized source at the other end.

The main advantage of this method is that the measurement time is very fast and the equipment can be easily used in the field. The dynamics and stability are provided by the well-established Fourier transform spectroscopy technique.

The fibre shall be single mode in the measured wavelength range.

The INTY method uses on two analyses that entail slightly different measurements:

The traditional analysis (TINTY) using a set of specific operating conditions for its successful applications and a basic set-up; and

A general analysis (GINTY) using no limiting operating conditions but using a modified set-up compared to TINTY.

5.1.3.2 Test apparatus

A generic set-up is shown in Figure 6 which is the basis of INTY experimental implementation. Variations of this set-up are possible and are shown below. The interferometer can be an air path type or a fibre type, it can be of Michelson or Mach-Zehnder type and it can be located at the source or at the detector end. Examples are given in Figures 7, 8 and 9.

NOTE – When a fibre-type interferometer is used, care should be given to the fibre chromatic dispersion that may add to the measurement uncertainties.

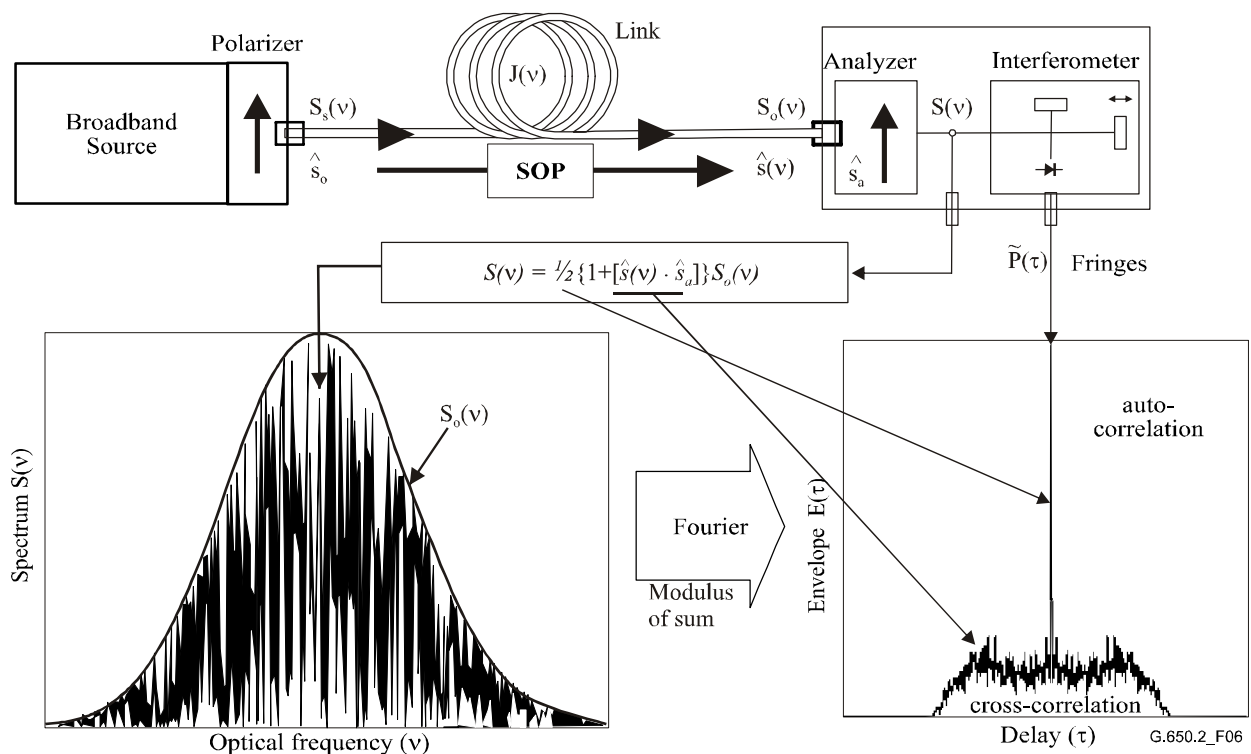


Figure 6/G.650.2 – Generic set-up for the interferometric technique

Parameters used in Figure 6 and later throughout this Recommendation:

- ν optical frequency ($\lambda\nu = c$);
- τ difference of round-trip delay between the two arms of the interferometer;
- $S_s(\nu)$ optical spectrum, at FUT input \equiv spectral density of $\vec{E}_s(\nu)$ the source electric field spectrum;
- $S_o(\nu)$ optical spectrum, at FUT output (analyser input);
- $S(\nu)$ optical spectrum, at analyser output (interferometer input);
- \hat{s}_0 input SOP (at FUT input; a unit Stokes vector);
- $\hat{s}(\nu)$ output SOP (at FUT output);
- \hat{s}_a analyser transmission axis;
- $\hat{s}(\nu) \cdot \hat{s}_a$ Stokes parameter giving the projection of $\hat{s}(\nu)$ on the analyser transmission axis. It is this parameter that contains the PMD information;
- $P(\tau)$ optical power at the interferometer output, as a function of delay τ ;
- $\tilde{P}(\tau)$ τ -dependent part of $P(\tau)$ ("a.c." part)
- P_0 constant part of $P(\tau)$ ("d.c." parts)
- $E(\tau)$ Fringe envelope
- $E_x(\tau)$ cross-correlation envelope
- $E_0(\tau)$ autocorrelation envelope

The optical power at the interferometer output, $P(\tau)$, is equal to the sum of "a.c." and "d.c." parts. Both parts are equal at $\tau = 0$ so the "a.c." part can be calculated. For an ideal interferometer, the "a.c." part is an even function, the right half of which is equal to the cosine Fourier transform of the optical spectrum, $S(\nu)$, emitted from the analyser. For non-ideal interferometers, some corrections may be applied, depending on the details of the implementation.

For TINTY, the envelope of the interferogram, $E(\tau)$, is the absolute value of the "a.c." part. For GINTY, additional calculations to obtain the cross-correlation and autocorrelation envelopes are described in 5.1.3.4.2. These calculations involve two measured interferograms resulting from the analyser being set at two orthogonal SOPs.

Other set-ups are shown below.

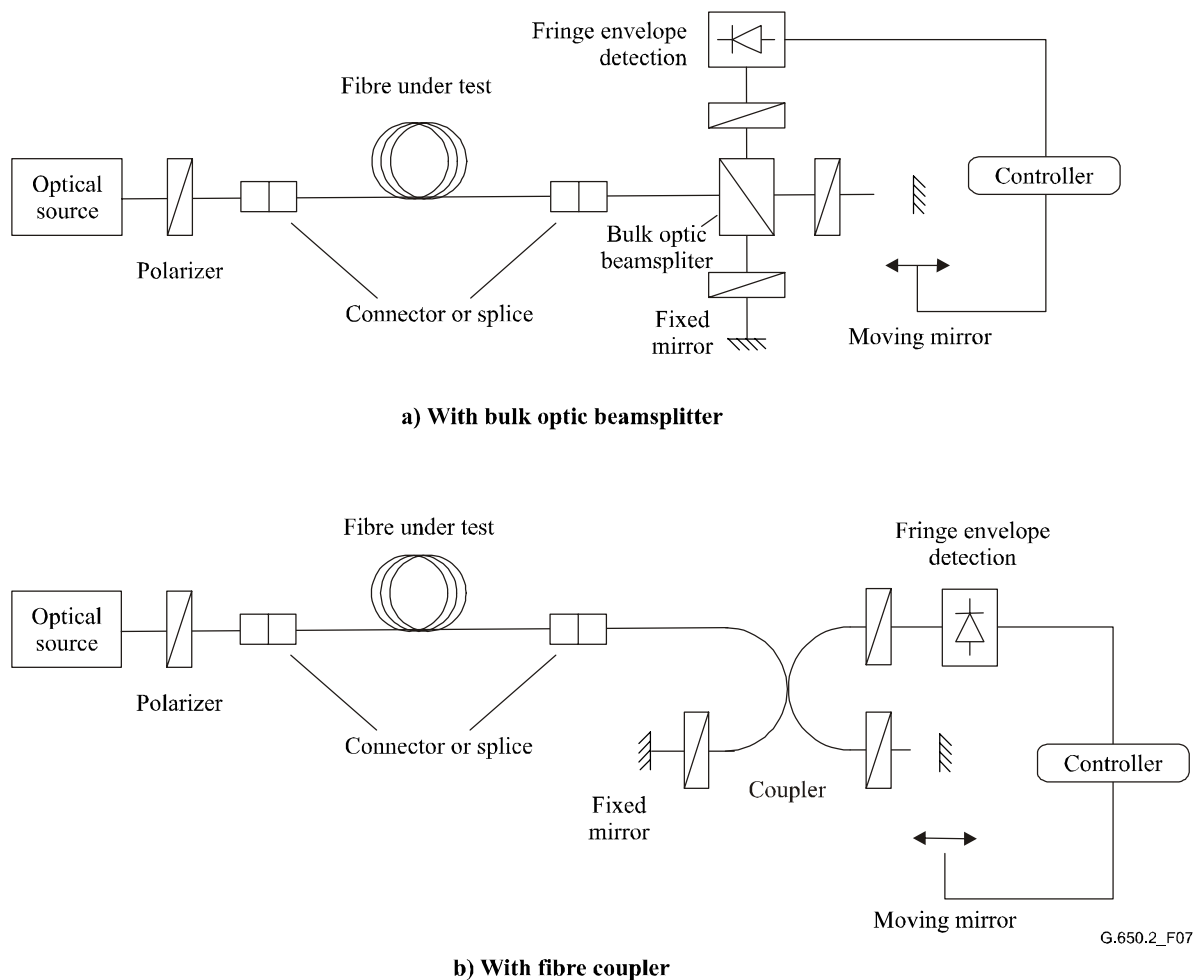


Figure 7/G.650.2 – The interferometric method using Michelson interferometer

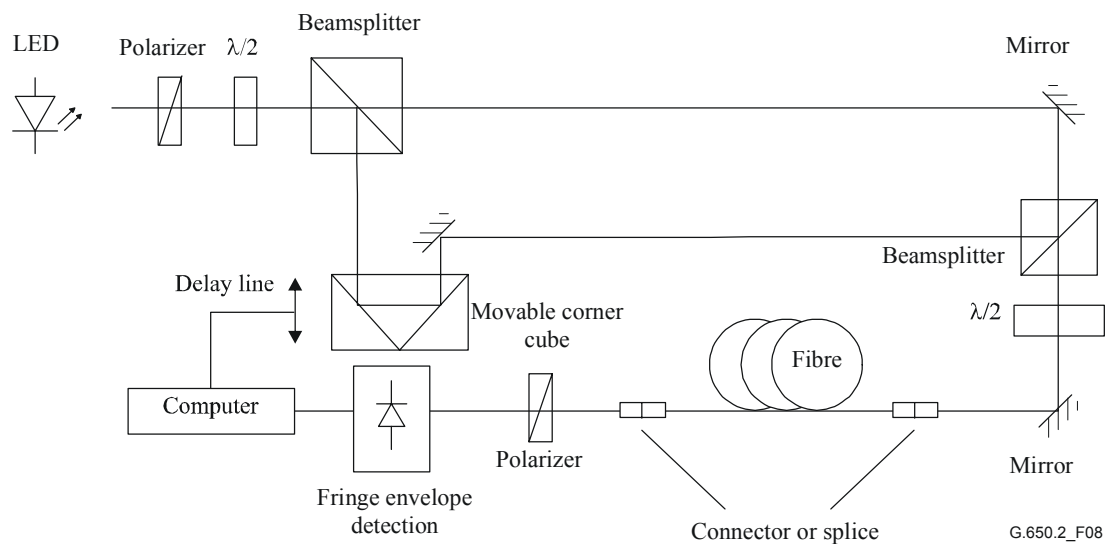


Figure 8/G.650.2 – The interferometric method using a Mach-Zehnder type interferometer with an air path

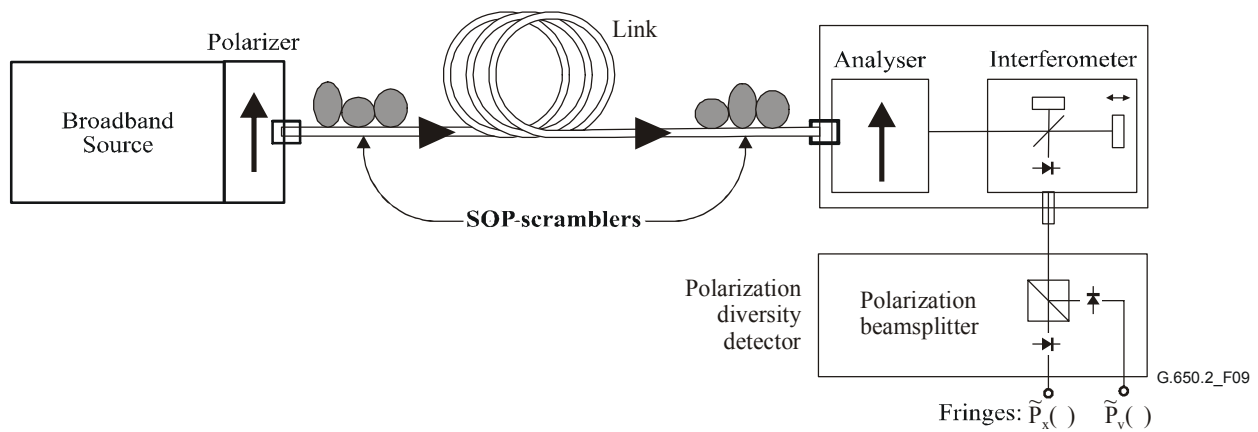


Figure 9/G.650.2 – The interferometric method (GINTY) using I/O-SOP scrambling and a polarization diversity detector

5.1.3.2.1 Optical source

A polarized broad spectrum source, such as a LED, set of super LED's or ASE source followed by a polarizer, shall be used. The centre wavelength of the light source shall be within the O-band and/or the C-band, or within any band of interest. A typical value of the source linewidth is about 60 nm or larger FWHM. TINTY requires that the spectral shape of the source shall be approximately Gaussian, without ripples which could influence the autocorrelation function of the emerging light. GINTY does not impose any such requirements. The source linewidth (also called spectral width in the LED field), $\Delta\lambda$, must be known to calculate the coherence time, t_c , which is determined with the following:

$$t_c = \frac{\lambda_0^2}{\Delta\lambda c} \quad (5-14)$$

where:

- λ_0 is the source centre wavelength;
- $\Delta\lambda$ is the source linewidth;
- c is the speed of light in vacuum.

5.1.3.2.2 Analyser

The analyser shall polarize the light over the full wavelength range of the source. For GINTY, the analyser must be capable of being rotated to a setting orthogonal to the initial setting.

5.1.3.2.3 Polarization scramblers (optional)

In Figure 9, the polarization scrambler allows the selection of any SOPs for the FUT input and output. The polarization beamsplitter allows simultaneous detection of what would be detected by two orthogonal analyser settings. The functionality of the polarization scrambler selecting various SOPs for the input and various analyser settings at the output can be achieved by other means.

5.1.3.2.4 Interferometer beamsplitter

The beamsplitter of the interferometer is used to split the incident polarized light into two components propagating in the interferometer's arms. The beamsplitter can be a fibre coupler as shown in Figure 7-b or a bulk optic beamsplitter as shown in Figure 7-a.

5.1.3.2.5 Detector

The light emerging from the FUT is coupled to a photodetector whose signal-to-noise ratio is adequate for the measurement. The detection system may include synchronous detection by chopper/lock-in amplifier or comparable techniques.

5.1.3.2.6 Computer

For the analysis of the interference pattern, a computer with suitable software shall be used.

5.1.3.3 Samples

The FUT sample shall be of known length of single-mode fibre which may or may not be cabled. The sample and pigtails must be fixed in position at a nominally constant temperature throughout the measurement. The standard ambient conditions shall be employed. In the case of installed fibres and cables, prevailing deployment conditions may be used.

It is important to minimize deployment-induced mode coupling when measuring uncabled fibres, which is done in order to support the primary requirements of cabled fibre PMD_Q. In this case, the fibre shall be supported in some manner (usually on a reel having a minimum wind radius of 150 mm), with essentially zero fibre tension (typically less than 5 g), and no tensioned crossovers. These deployment requirements can limit the length that can be measured, depending on the spool diameter, and can make the measurement a destructive one. Multi-layer windings are possible, but should be qualified by comparison with single-layer results on shorter lengths.

The measurement of uncabled fibre deployed on shipping spools is not recommended. PMD results with this deployment have been shown to be substantially less than what would be obtained in cable form for high PMD fibre and substantially greater than what would be obtained in cable form for low PMD fibre.

NOTE – Although the test sample is normally a fibre, this test can also be performed on discrete components. In this case, PMD coefficient is not relevant. However, in the case of TINTY, the PMD resolution will always be limited by the width of the autocorrelation peak (typically in the 100-fs range). GINTY does not suffer from such limitations and PMD resolutions only limited by the instrument implementation uncertainties can be achieved (typically in the 10-fs range or less).

5.1.3.4 Procedure

One end of the FUT is coupled to the polarized output of the polarized light source. The other end is coupled to the output optics. This can be done by standard fibre connectors, splices or by a fibre alignment system. If the latter is used, some index matching oil should be used to avoid reflections.

The optical output power of the light source is adjusted to a reference value characteristic for the detection system used. To get a sufficient fringe contrast, the optical power in both arms shall be almost identical.

5.1.3.4.1 TINTY procedure

Make a first acquisition in moving the mirror of the interferometer arm and recording the intensity of the light. Subtract the value found for $\tau = 0$ from the interferogram to obtain $\tilde{P}(\tau)$. The absolute value of $\tilde{P}(\tau)$ is the fringe envelope, $E(\tau)$.

From the obtained fringe pattern for one selected state of polarization, the PMD delay can be calculated as described below. Typical example of a fringe pattern for low and high polarization mode coupling is shown in Figure 10.

In case of insufficient mode coupling or in case of low PMD, it is recommended to repeat the measurement for different SOPs or to modulate the SOP during the measurement in order to obtain a result which is an average over all SOPs.

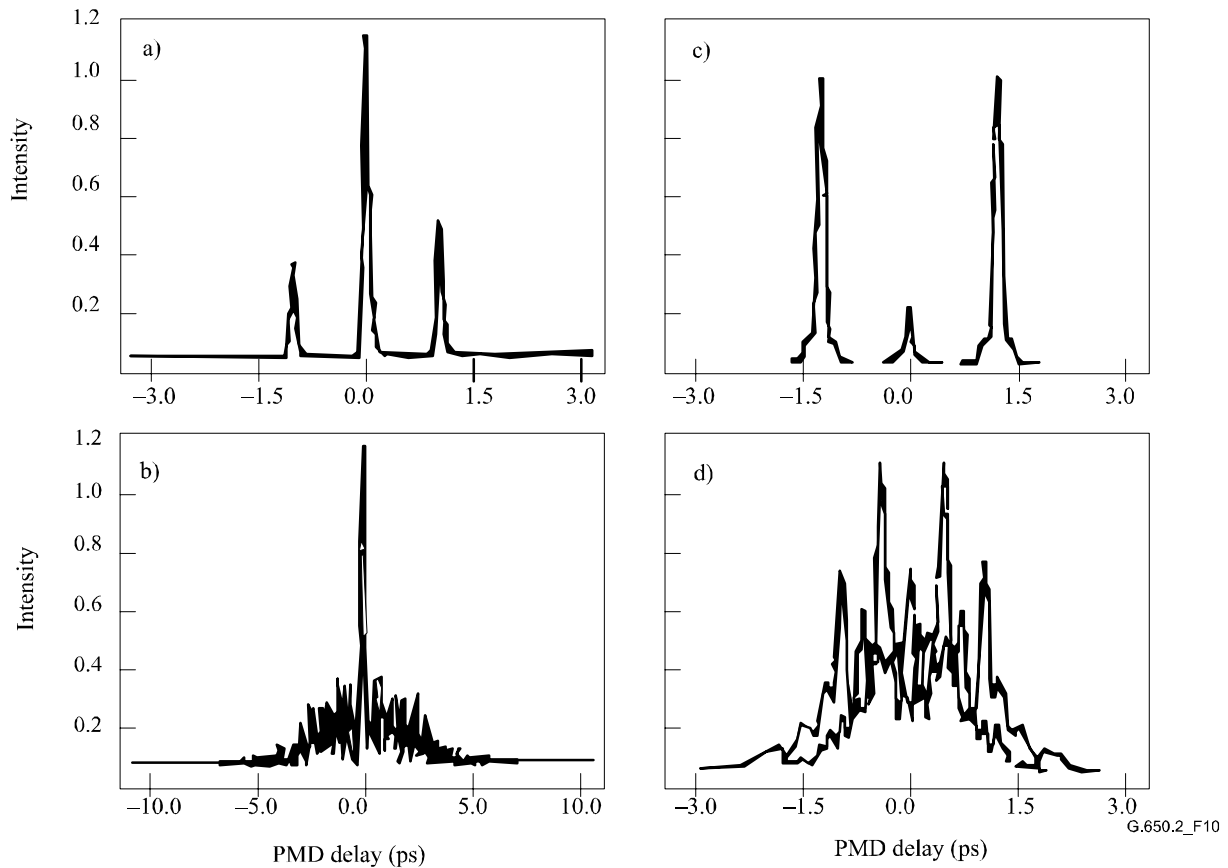


Figure 10/G.650.2 – Example of a fringe patterns obtained with the autocorrelation type instrument (a, b) and with the cross-correlation type instrument (c, d) for negligible (top) and random (bottom) polarization mode coupling

The fringe envelopes obtained from TINTY are a combination of the cross-correlation and autocorrelation functions. An algorithm must be used to try to separate out the part that is from the cross-correlation function.

5.1.3.4.2 GINTY procedure

The combination of a particular input polarizer setting and an orthogonal pair of analyser settings is called an I/O SOP. Complete the scan(s) for the two interferograms and subtract the "d.c." part from each to obtain $\tilde{P}_x(\tau)$ and $\tilde{P}_y(\tau)$, the orthogonally generated fringes.

The cross-correlation and autocorrelation fringe envelopes, $E_x(\tau)$ and $E_0(\tau)$ are calculated as:

$$E_x(\tau) = |\tilde{P}_x(\tau) - \tilde{P}_y(\tau)| \quad E_0(\tau) = |\tilde{P}_x(\tau) + \tilde{P}_y(\tau)| \quad (5-15)$$

These functions are squared for the purposes of later calculations and display. Some example squared cross-correlation results are shown below. Note that the autocorrelation peak seen with the TINTY is not present.

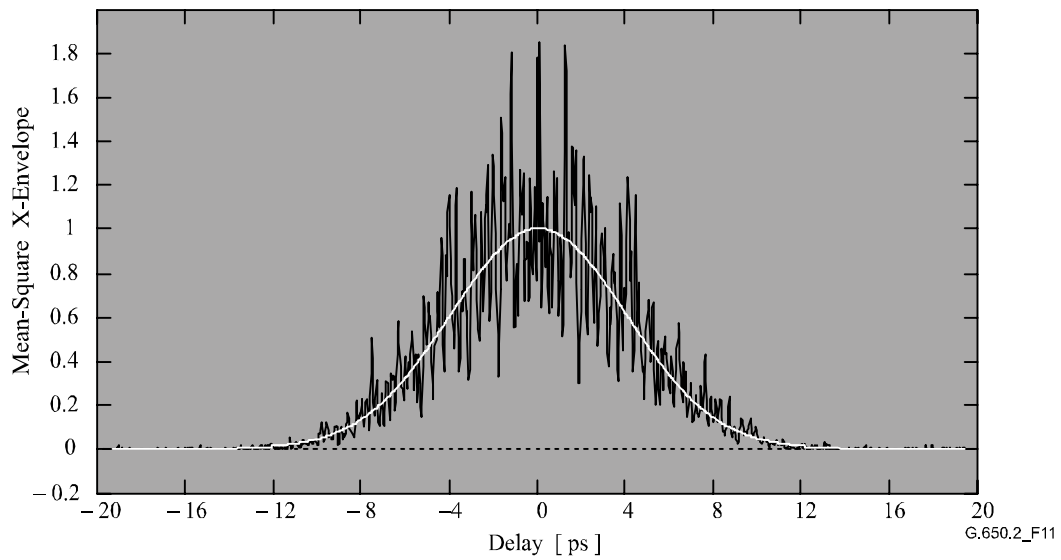


Figure 11/G.650.2 – Example of a fringe pattern obtained with GINTY and I/O-SOP scrambling for random mode coupling

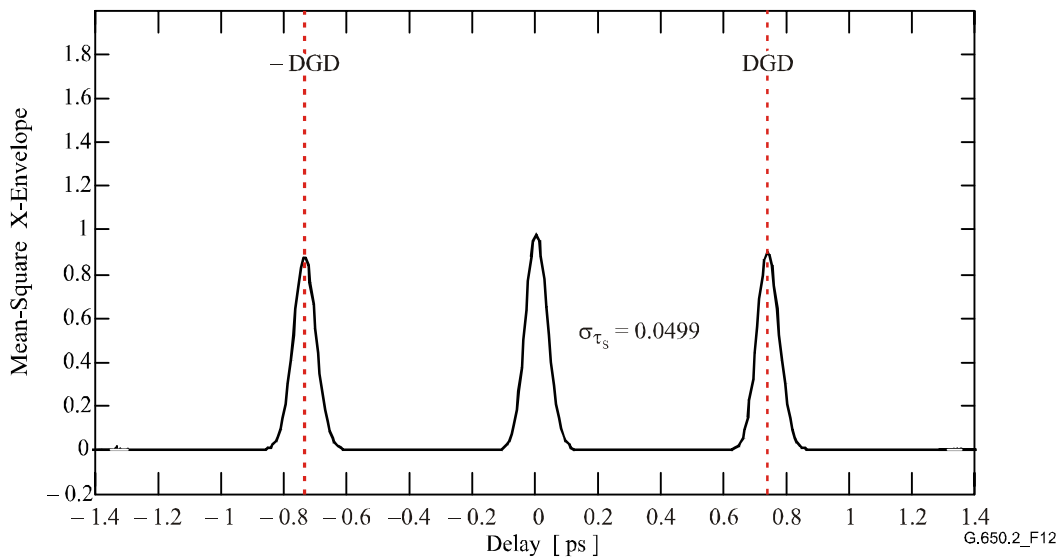


Figure 12/G.650.2 – Example of a fringe pattern obtained with GINTY and I/O-SOP scrambling for negligible mode coupling

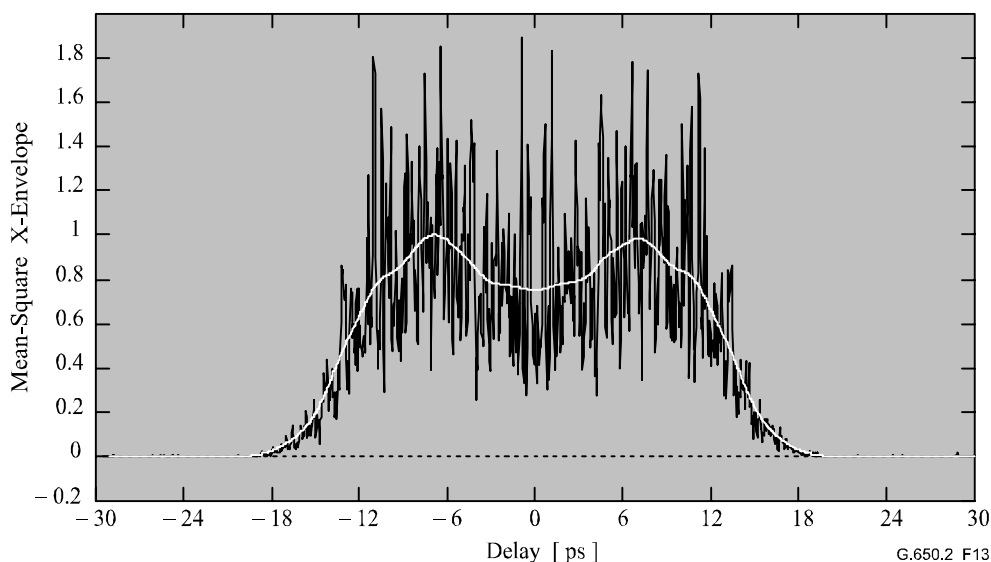


Figure 13/G.650.2 – Example of a fringe pattern obtained with GINTY and I/O-SOP scrambling for mixed mode coupling

Options for polarization scrambling follow. When multiple I/O SOPs are measured, index them with *i* for later calculations.

5.1.3.4.2.1 The 9-states Mueller set

The sum of nine squared envelopes observed with nine specific I/O SOPs is rigorously equal to the uniformly scrambled mean squared envelope. These nine I/O SOPs are: three analyser-axes forming a right-angled trihedron, for each three input SOPs also forming a right-angled trihedron.

5.1.3.4.2.2 Random scrambling

- Scan-to-scan scrambling: automatic/manual setting of the scramblers at each scan.
- Continuous scrambling: when squared envelopes are summed, scrambling can be performed while scanning. Automated scramblers are set to cover the sphere continuously as a function of time.
- Fast, single-scan scrambling: if scramblers are sufficiently fast, well-scrambled squared envelopes can be observed in a single-scan. However, this requires special provisions to avoid crosstalk between the a.c. part and the previously d.c. part of the interferogram.

5.1.3.5 Calculations

Both these calculations report PMD_{RMS} . For ideal random mode coupling when the interferogram is of an ideal Gaussian shape, this may be converted to PMD_{AVG} using Equation 3-3.

5.1.3.5.1 TINTY calculations

For the case of negligible mode coupling, the separation of the single well-defined peaks from the centre is the DGD value, which is also the PMD value.

The following calculations are suitable for the random mode-coupling regime associated with long fibres/cables or links. The spread in the fringe envelope, discounting the centre peak, is characterized.

The PMD_{RMS} value is determined from the second moment (RMS width) of the cross-correlation function of the detected signal (fringe envelope).

$$PMD_{RMS} = \left(\sqrt{\frac{3}{4}} \right) \sigma_{\epsilon} \quad (5-16)$$

where:

σ_{ϵ} is the RMS width of the cross-correlation envelope.

A detailed algorithm for the calculation of σ_{ϵ} from a measured fringe envelope is described in Appendix I.1.

For certain assumptions given below, Equation 5-14 can be related to Equation 3-2 as:

$$\langle \Delta\tau^2 \rangle = \frac{3}{4} \langle \sigma_{\epsilon}^2 \rangle \quad (5-17)$$

Equation 5-12 is obtained from the theory given the following assumptions:

- Ideal random mode coupling;

NOTE 1 – Ideal random coupling means $L/h \rightarrow \infty$, and a uniformly distributed birefringence axis. L is the device length and h is the polarization coupling-length. For a device consisting of N concatenated birefringent segments of length h , this corresponds to $N \rightarrow \infty$ with uniformly distributed axes.

NOTE 2 – Analysis of no (or negligible) mode coupling is possible.

- A purely Gaussian source, with no ripples;
- $PMD \gg \sigma_0$

where:

σ_0 is the RMS width of the auto-correlation envelope;

- Ergodic conditions.

NOTE 3 – Given that the source is Gaussian, the result must be some form of weighted average of the DGD values. This weighting is not specified in TINTY, but is in GINTY. For this reason, this method is expected to give a different result for a given wavelength range and time than one of the methods that use a rectangular weighting (such as for example, the RTM). The assumption of ergodic conditions does result in the validity of the expected value relationship. In practice, the wavelength ranges sampled by different implementations of the other methods will also vary which would imply getting different results between them as well.

5.1.3.5.2 GINTY calculations

GINTY allows some of the assumptions required for Equation 5-16 with TINTY to be removed. Notably:

- The assumption of ideal random mode coupling is not required;
- The assumption of a Gaussian source is not required;
- The assumption that the PMD is large compared to the width of the autocorrelation function is not required.

Form the mean squared cross-correlation and autocorrelation envelopes, $\bar{E}_x^2(\tau)$ and $\bar{E}_0^2(\tau)$ as:

$$\bar{E}_x^2(\tau) = \frac{1}{N} \sum_i E_{xi}^2(\tau) \quad \bar{E}_0^2(\tau) = \frac{1}{N} \sum_i E_{0i}^2(\tau) \quad (5-18)$$

where N is the number of I/O SOPs.

Calculate the RMS width of the two sampled mean squared envelopes, σ_0 and σ_x , respectively. A sample algorithm for this calculation is given in Appendix I.2. The mathematical definitions of these widths are:

$$\sigma_x^2 = \frac{\int \tau^2 \langle E_x^2(\tau) \rangle d\tau}{\int \langle E_x^2(\tau) \rangle d\tau} \quad \sigma_0^2 = \frac{\int \tau^2 \langle E_0^2(\tau) \rangle d\tau}{\int \langle E_0^2(\tau) \rangle d\tau} \quad (5-19)$$

The expected value operator in the above equations is with respect to a uniform and random sampling of the I/O-SOPs.

The PMD_{RMS} value that is reported is:

$$PMD_{RMS} = \left[\frac{3}{2} (\sigma_x^2 - \sigma_0^2) \right]^{1/2} \quad (5-20)$$

Equation 5-20 relates to Equation 3-2 as:

$$\frac{\int \Delta\tau^2(\nu) S_0^2(\nu) d\nu}{\int S_0^2(\nu) d\nu} = \frac{3}{2} (\sigma_x^2 - \sigma_0^2) \quad (5-21)$$

Using the ideal definitions of the RMS width terms from Equation 5-19, Equation 5-21 is exact for any DGD curve present at the time of measurement and any source spectral characteristics. The left side of Equation 5-21 is a spectrally weighted (by squared power) RMS calculation.

Using the assumption of ergodic conditions:

$$\langle \Delta\tau^2 \rangle = \left\langle \frac{\int \Delta\tau^2(\nu) S_0^2(\nu) d\nu}{\int S_0^2(\nu) d\nu} \right\rangle \quad (5-22)$$

5.1.3.6 Presentation of the results

- a) Date.
- b) Fibre identification.
- c) Fibre type.
- d) Fibre length.
- e) Test set-up arrangement, including source type, wavelength, linewidth (FWHM).
- f) Launching technique.
- g) Type of fringe detection technique.
- h) Plot over the scanned range with fringe pattern (only if mode coupling type is not random).
- i) Fibre deployment and environmental conditions (radius, stress, temperature, etc.).
- j) Mode coupling type (random, mixed or negligible).
- k) Analysis method (TINTY or GINTY)
- l) PMD_{RMS} (ps) or PMD_{AVG} (specify which) (ps), and PMD coefficient. If the degree of mode coupling is known, the coefficient may be given in ps/km or ps/ $\sqrt{\text{km}}$.

5.1.4 The fixed analyser technique

5.1.4.1 General

This test method describes a procedure for measuring the Polarization Mode Dispersion (PMD) of single-mode optical fibres. It produces a single measurement value that represents the PMD over the measurement wavelength range of typically a few hundred nanometers. The method can be applied to both short and long fibres in the limits of both zero and strong polarization mode coupling. Under some circumstances, repeated measurements may be necessary to achieve

satisfactory precision using this method. The procedure is restricted to wavelengths greater than or equal to that at which the fibre is effectively single-mode.

5.1.4.2 Test apparatus

See Figure 14 for a schematic diagram of the key components in a typical measurement system.

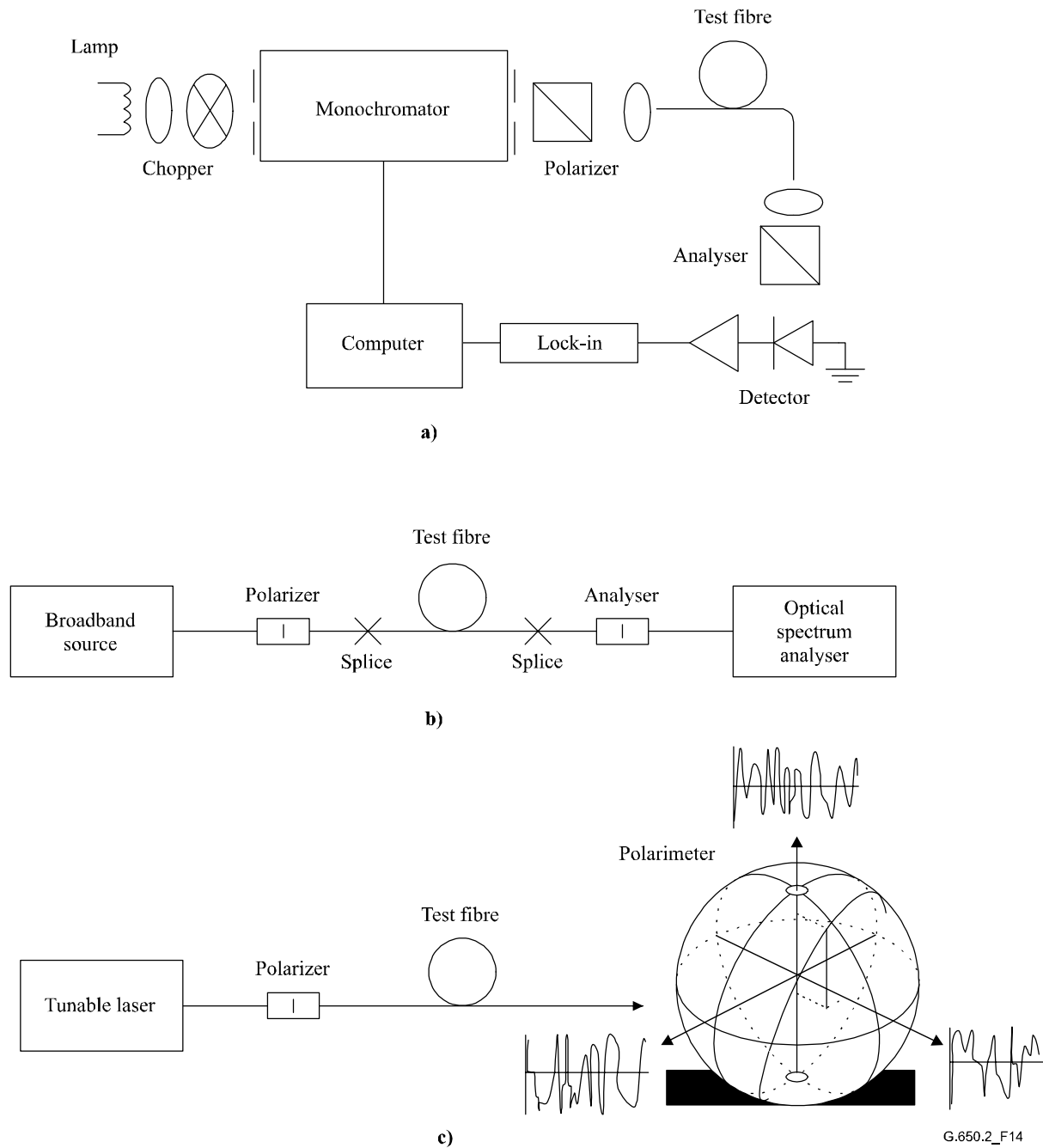


Figure 14/G.650.2 – Schematic diagram of equipment (typical)

5.1.4.2.1 Light source

Use a light source which emits radiation at the intended measurement wavelengths, such as a broadband lamp, light emitting diode(s) or tunable laser(s). It shall be stable in intensity and spectral distribution over a time period long enough to perform the measurement.

5.1.4.2.2 Monochromator

Obtain a specified set of test wavelengths by filtering the light source with a monochromator as in Figure 14-a, or by using an optical spectrum analyser as the detector, as in Figure 14-b. This filtering is not needed when the source is a tunable laser (see Figure 14-c). The spectral distribution must be narrow enough to avoid major depolarization of the signal under the influence of the PMD of the fibre under test (see 5.1.4.4.1.4 and 5.1.4.4.2.8).

5.1.4.2.3 Input optics

An optical lens system or single-mode fibre pigtail may be employed to excite the test fibre. The power coupled into the fibre shall be stable for the duration of the test. If pigtails are used, interference effects due to reflections should be avoided. This may require index matching materials or angled cleaves. The pigtails shall be single-mode.

If an optical lens system is used, some suitable means, such as a vacuum chuck, shall be used to stably support the input end of the fibre.

5.1.4.2.4 Cladding mode stripper

Remove any cladding mode power from the test fibre. Under most circumstances, the fibre coating will perform this function; otherwise, employ a device that extracts cladding mode power.

5.1.4.2.5 Output optics

All power emitted from the test fibre must be coupled onto the active region of the detection system (see Figure 14). An optical lens system, a butt splice to a single-mode fibre pigtail or an index-matched fibre-to-fibre coupling made directly to the detection system are examples of means that may be used.

5.1.4.2.6 Signal detection

For signal detection, use an optical detector which is linear and stable over the range of intensities and measurement times that are encountered in performing the measurement. A typical system might include synchronous detection by a chopper/lock-in amplifier, an optical power meter, an optical spectrum analyser or a polarimeter. To use the entire spectral range of the source, the detection system must have a wavelength range which includes the wavelengths produced by the light source.

5.1.4.2.7 Polarizer and analyser

The polarizer at the fibre input (Figure 14) is needed only if the launch beam is not already polarized (usually a 3 dB extinction ratio is sufficient). The angular orientation of the polarizers is not critical, but should remain fixed throughout the measurement. With weak mode coupling, some adjustment of the polarizer orientation may be helpful in maximizing the amplitude of the oscillations in Figure 15-a. Alternatively, this may be achieved by rotation of the fibre(s) at splices or connectors.

The analyser is not needed when a polarimeter is used for signal detection (Figure 14-c).

5.1.4.3 Measurement procedure

The test sample shall be a known length of a single-mode optical fibre which may or may not be cabled. The sample and pigtails must be fixed in position at a nominally constant temperature throughout the measurement.

NOTE – Although the test sample is normally a fibre, this test can also be performed on discrete components. In this case, PMD coefficient is not relevant.

Temperature stability of the test device may be observed by measuring the output power from the fibre at a fixed wavelength, with the output analyser in place. In a time period corresponding to a typical complete measurement, the output power change should be small relative to the changes produced by a wavelength increment.

It is important to minimize deployment induced mode coupling when measuring uncabled fibres, which is done in order to support the primary requirements of cabled fibre PMD₀. In this case, the fibre shall be supported in some manner (usually on a reel having a minimum wind radius of 150 mm), with essentially zero fibre tension (typically less than 5 g), and no tensioned crossovers. These deployment requirements can limit the length that can be measured, depending on the spool diameter, and can make the measurement a destructive one. Multi-layer windings are possible, but should be qualified by comparison with single-layer results on shorter lengths.

The measurement of uncabled fibre deployed on shipping spools is not recommended. PMD results with this deployment have been shown to be substantially less than what would be obtained in cable form for high PMD fibre and substantially greater than what would be obtained in cable form for low PMD fibre.

Couple the input end of the fibre to the light source. Couple the output radiation from the fibre under test to the detection system.

By making appropriate adjustments to the monochromator, optical spectrum analyser or tunable laser, inject each designated test wavelength λ in turn into the fibre. The choice of wavelengths depends on the designated wavelength scan range and also on the analysis method (see 5.1.4.4.1 and 5.1.4.4.2).

Record the corresponding output signal for each wavelength. This process shall be accomplished without changing the launch and detector conditions. Call the received power $P_A(\lambda)$, where A denotes the presence of the analyser.

Remove the analyser from the beam and repeat the monochromator scan. Call this received power $P_{TOT}(\lambda)$. This latter power can be used to eliminate the spectral dependence of the measurement system components and the test fibre loss. Typical plots of the ratio:

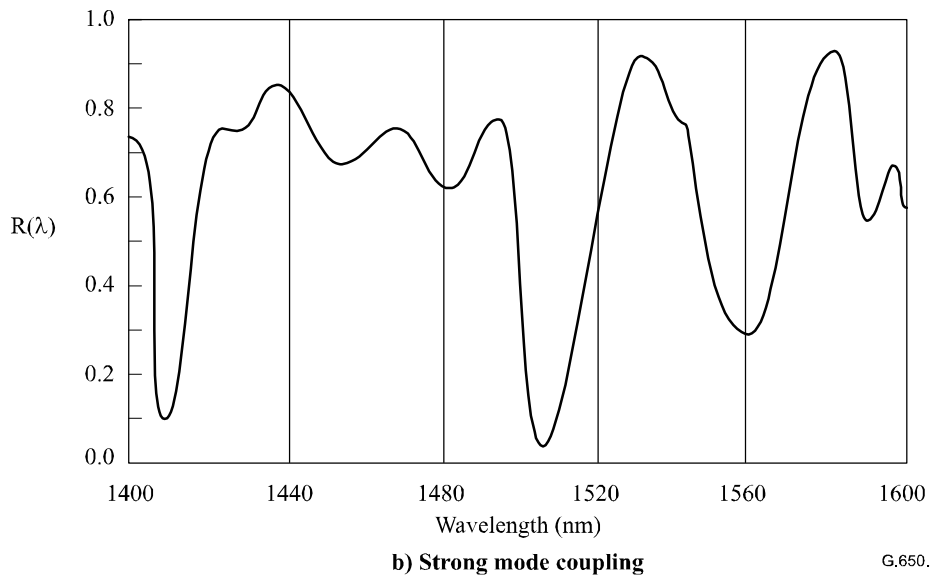
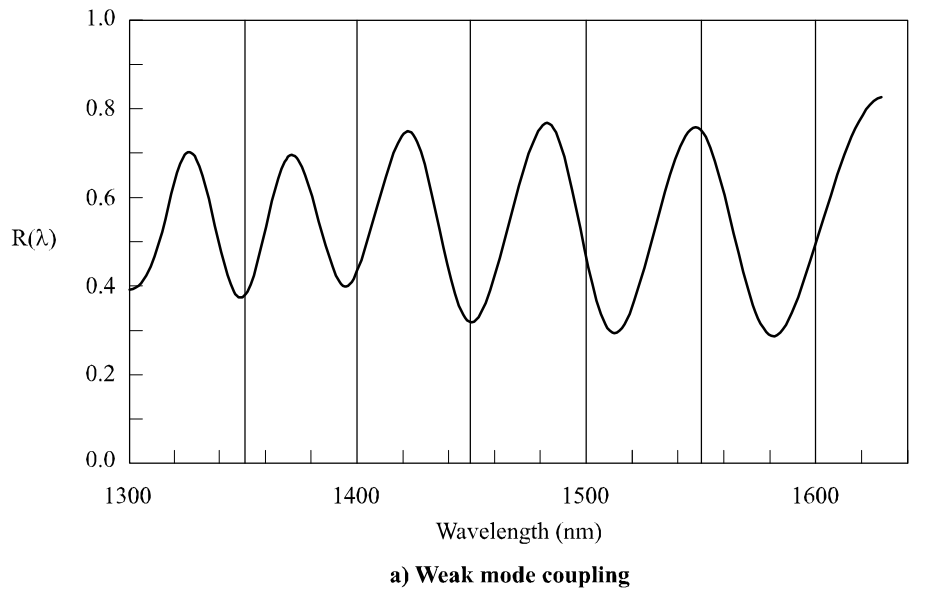
$$R(\lambda) = \frac{P_A(\lambda)}{P_{TOT}(\lambda)} \quad (5-23)$$

are shown in Figure 15.

An alternative procedure is to leave the analyser in place, but rotate it 90° with respect to the orientation used above. Calling the power received in this case $P_{ROT}(\lambda)$, then:

$$R(\lambda) = \frac{P_A(\lambda)}{P_A(\lambda) + P_{ROT}(\lambda)} \quad (5-24)$$

If a polarimeter is used as the detection element, the normalized Stokes parameters are measured versus wavelength. The three spectral functions are independent of the received power and are analysed by the same methods applied to $R(\lambda)$ (see 5.1.4.4.1 and 5.1.4.4.2). Each normalized Stokes parameter then leads to a value of $\langle \Delta\tau \rangle$.



G.650.2_F15

Figure 15/G.650.2 – Typical data obtained in measuring PMD

5.1.4.4 Calculations or interpretation of results

One of the following two methods (5.1.4.4.1 and 5.1.4.4.2) shall be used for calculating PMD from the measurement data.

5.1.4.4.1 Extrema counting

5.1.4.4.1.1 PMD

$R(\lambda)$ should be obtained at evenly spaced wavelength intervals. E is the number of extrema within the window $\lambda_1 < \lambda < \lambda_2$. Alternatively, λ_1 and λ_2 may be chosen to coincide with extrema, in which case E is the number of extrema (including the ones at λ_1 and λ_2) minus one.

$$\langle \Delta\tau \rangle = \frac{k E \lambda_1 \lambda_2}{2(\lambda_2 - \lambda_1)c} \quad (5-25)$$

where c is the speed of light in vacuum, k is a mode coupling factor which equals 1.0 in the absence of mode coupling (the Equation 3-4 regime) and 0.82 in the limit of strong mode coupling (the

Equation 3-5 regime).

If a polarimeter is used as the detection element, take as the final value of $\langle \Delta\tau \rangle$ the average of the values derived from the three normalized Stokes parameter responses. The resulting value is to be interpreted as an average over the wavelength range $\lambda_1 < \lambda < \lambda_2$.

5.1.4.4.1.2 Accuracy

The best accuracy is obtained by making $(\lambda_2 - \lambda_1)$ large enough to insure that $E \gg 1$. This is especially important when there is strong mode coupling (Figure 15-b) and less so otherwise (Figure 15-a). Values of E in the range of 7 to 40 are typical. When E is at the low end of this range, the percentage of uncertainties in both E and the PMD become large. At the upper end of the range, instrumental broadening may result in some adjacent peaks not being resolved.

Ideally, the scan window should be centered on the fibre's wavelength of use, and the window made wide enough to ensure that E is greater than about 10 for the maximum PMD value of interest (where pass/fail is an issue).

5.1.4.4.1.3 Peak identification

The identification of extrema in $R(\lambda)$ can be more difficult in the presence of noise and/or strong mode coupling. This can be seen in the example of Figure 15-b. An algorithm with the following features is useful in identifying extrema:

- 1) A polynomial is fitted to several adjacent points of $R(\lambda)$ to provide a smoothed curve.
- 2) An extremum is defined as a point where the wavelength derivative of this smoothed curve changes sign.

Additional robustness can be built into the peak identification algorithm if needed.

5.1.4.4.1.4 Spectral resolution

To insure that all features in the optical spectrum are adequately resolved, the spectral resolution $\Delta\lambda$ should satisfy:

$$\Delta\lambda / \lambda < (8\nu\Delta\tau)^{-1} \quad (5-26)$$

where ν is the optical frequency. $\Delta\lambda$ is the instrumental spectral width or the wavelength step size, whichever is larger. For λ in the vicinity of 1550 nm, Equation 5-26 reduces to the condition that $\Delta\lambda$ (nm) should be less than the reciprocal of $\Delta\tau$ (ps).

5.1.4.4.2 Fourier analysis

5.1.4.4.2.1 Overview

In this method, a Fourier analysis of $R(\lambda)$, usually expressed in the domain of optical frequency, ν , is used to derive PMD. The Fourier transform transforms this optical frequency domain data to the time domain. The Fourier transform yields direct information on the distribution of light arrival times $\delta\tau$. This data is post-processed as described below to derive the expected PMD, $\langle \Delta\tau \rangle$, for the fibre under test. This method is applicable to fibres with weak or strong mode coupling (refer to 5.1.4.4.2.4 and 5.1.4.4.2.5, respectively).

5.1.4.4.2.2 Data preprocessing and Fourier transformation

To use this method, the Fourier transform normally requires equal intervals in optical frequency so that $R(\lambda)$ data is collected (as described in 5.1.4.3) at λ values such that they form equal intervals in the optical frequency domain. Alternatively, data taken at equal λ intervals may be fitted (for example, by using a cubic spline fit) and interpolation used to generate these points, or more advanced spectral estimation techniques used. In each instance, the ratio $R(\lambda)$ at each λ value used

is calculated using Equations 5-23 or 5-24 as appropriate.

Zero-padding or data interpolation and DC level removal may be performed on the ratio data, $R(\lambda)$. Windowing the data may also be used as a preconditioning step before the Fourier transform. The Fourier transformation is now carried out to yield the amplitude data distribution $P(\delta\tau)$ for each value of $\delta\tau$.

5.1.4.4.2.3 Transform data fitting

Fourier transformed data at zero $\delta\tau$ has little meaning since, unless carefully removed, DC components in $R(\lambda)$ may be partially due to insertion loss of the analyser, for example. When the DC level is not removed, up to two data points are generally bypassed (not used) in any further calculations. A variable, j , is defined so that the "first valid bin" above zero $\delta\tau$ that is included in calculations corresponds to $j = 0$.

In order to remove measurement noise from subsequent calculations, $P(\delta\tau)$ is compared to a threshold level T_1 , typically set to 200% of the r.m.s. noise level of the detection system. It is now necessary to determine whether the fibre is weakly or strongly mode coupled.

If it is found that the first X valid points of $P(\delta\tau)$ are all below T_1 , this indicates that $P(\delta\tau)$ must have discrete spike features characteristic of weakly coupled fibres. The value of X is equal to three, unless zero-padding is used in the Fourier analysis. In that case, the value of X can be determined from $3 \times (\text{number of original data points}) / (\text{total length of array after zero-padding})$. Use clause 5.1.4.4.2.4 to calculate PMD. If this is not the case, proceed to calculate PMD using clauses 5.1.4.4.2.5 or 5.1.4.4.2.6.

5.1.4.4.2.4 PMD calculation for fibres with weak mode coupling

For a weakly coupled fibre (e.g., a high birefringence fibre) or for a birefringent component, $R(\lambda)$ resembles a chirped sine wave (Figure 15-a). Fourier transformation will give a $P(\delta\tau)$ output containing a discrete spike at a position corresponding to the relative pulse arrival time, $\delta\tau$, the centroid of which is the PMD value $\langle\Delta\tau\rangle$.

To define the spike centroid $\langle\Delta\tau\rangle$, those points where $P(\delta\tau)$ exceeds a second predetermined threshold level T_2 , typically set to 200% of the r.m.s. noise level of the detection system, are used in the equation:

$$\langle\Delta\tau\rangle = \frac{\sum_{e=0}^{M'} [P_e(\delta\tau)\delta\tau_e]}{\sum_{e=0}^{M'} [P_e(\delta\tau)]} \quad (5-27)$$

where $M' + 1$ is the number of data points of P within the spike which exceed T_2 . $\langle\Delta\tau\rangle$ in Equation 5-15 is typically quoted in picoseconds. If the device under test is a fibre of length L , the PMD coefficient may be calculated using Equation 3-4. If no spike is detected (i.e., $M' = 0$), then PMD is zero. Other parameters such as the r.m.s. spike width and/or spike peak value may be reported.

If the device under test contains one or more birefringent elements, more than one spike will be generated. For a number n concatenated fibres/devices, $2^{(n-1)}$ spikes will be obtained.

5.1.4.4.2.5 PMD calculation for fibres with strong mode coupling

In instances of strong mode coupling, $R(\lambda)$ becomes a complex waveform similar to Figure 15-b, the exact characteristics being based on the actual statistics of the coupling process within the fibre/cable. The Fourier transformed data now becomes a distribution $P(\delta\tau)$ representing the autocorrelation of the probability distribution of light pulse arrival times, $\delta\tau$, in the fibre.

Counting up from $j = 0$, determine the first point of P which exceeds T_1 , and which is followed by at least X data points which fall below T_1 . This point represents the last significant point (i.e., the "end" of) the distribution $P(\delta\tau)$, for a strongly mode-coupled fibre, that is not substantially affected by measurement noise. The $\delta\tau$ value for this point is denoted $\delta\tau_{last}$, and the value of j at $\delta\tau_{last}$ is denoted M'' . This fibre is strongly mode coupled. The square root of the second moment, σ_R , of this distribution defines the fibre PMD $\langle\Delta\tau\rangle$, and is given by:

$$\langle\Delta\tau\rangle = \sigma_R = \left\{ \frac{\sum_{j=0}^{M''} [P_j(\delta\tau)\delta\tau_j^2]}{\sum_{j=0}^{M''} [P_j(\delta\tau)]} \right\}^{1/2} \quad (5-28)$$

The $\langle\Delta\tau\rangle$ value given by Equation 5-28 is typically quoted in picoseconds. An example of the Fourier transform output obtained in a 25 km fibre with strong mode coupling is shown in Figure 16.

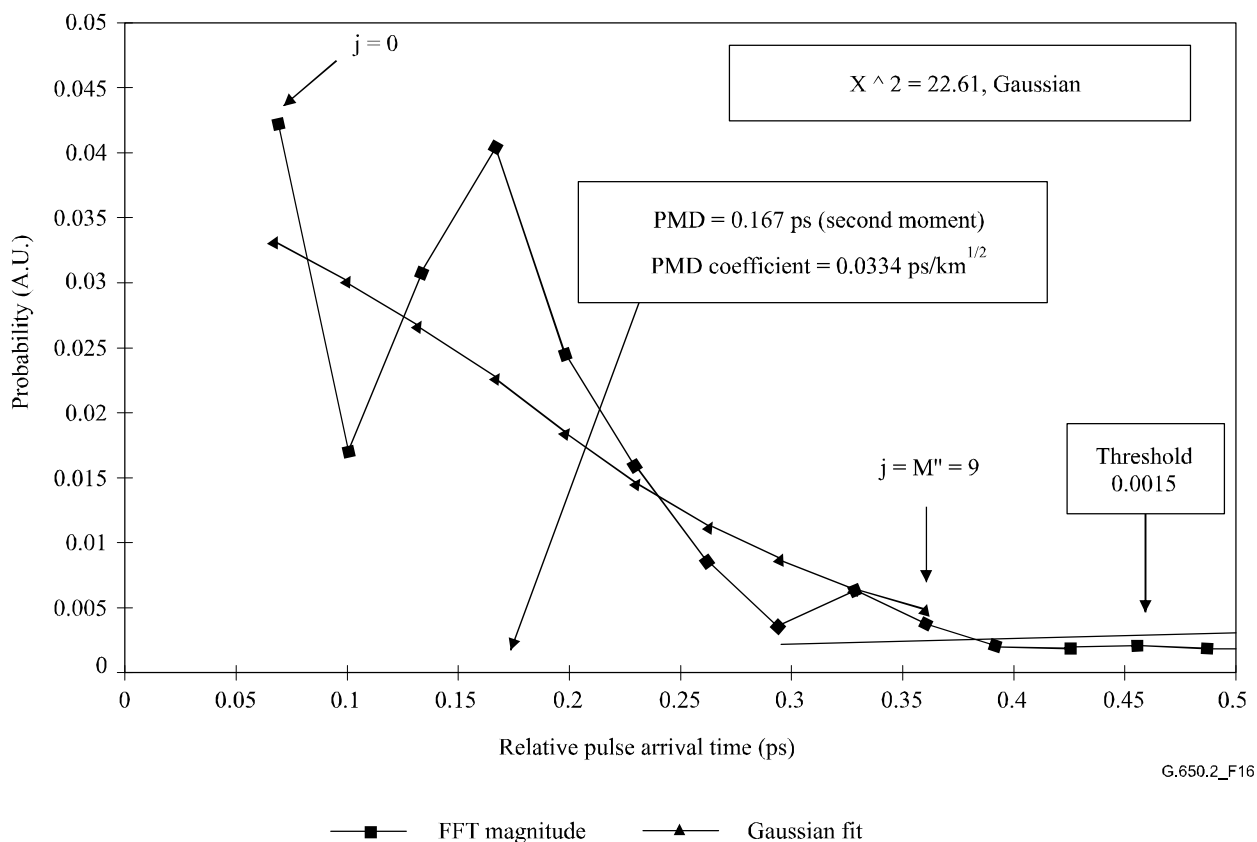


Figure 16/G.650.2 – PMD using Fourier analysis

5.1.4.4.2.6 PMD calculation for mixed coupling fibre systems

There may be instances where both weakly coupled fibre/components and strongly coupled fibre(s) are concatenated to form the system under test. In this case, both centroid determination (5.1.4.4.2.4) and the second moment derivation (5.1.4.4.2.5) may be required. Note that spikes in $P(\delta\tau)$ may only be determined beyond the $\delta\tau_{last}$ computed.

5.1.4.4.2.7 Spectral range

For strongly coupled fibres, sufficient spectral range must be used to form the spectral ensemble (average) with sufficient precision. The statistical uncertainty may be minimized by using the widest possible spectral range (e.g., at least 200 nm). The precision required and therefore spectral

range must be specified prior to the measurement. The maximum usable range is limited by the fibre cut-off wavelength (1270 nm or below) at the short (λ_1) end, and by the detector responsivity roll-off at the high (λ_2) end (e.g., 1700 nm).

In addition, very low $\delta\tau$ values will give very long periods in $R(\lambda)$, and the spectral range λ_1 to λ_2 must cover at least two complete "cycles". The spectral range covered defines the smallest $\delta\tau$ value that can be resolved in $P(\delta\tau)$, $\delta\tau_{\min}$:

$$\delta\tau_{\min} = \frac{2\lambda_1\lambda_2}{(\lambda_2 - \lambda_1)c} \quad (5-29)$$

where the factor 2 is introduced to allow for the fact that two data points in P at and adjacent to zero are generally ignored (see 5.1.4.4.2.3). For example, for $\lambda_1 = 1270$ nm, $\lambda_2 = 1700$ nm, $\delta\tau_{\min} = 0.033$ ps.

For weakly coupled high PMD fibres with ratio data $R(\lambda)$ resembling Figure 15-a, the requirement for spectral averaging described above may be relaxed, and the spectral range reduced [e.g., $(\lambda_2 - \lambda_1) \sim 30$ nm] in order to allow variation of PMD with wavelength to be examined.

5.1.4.4.2.8 Wavelength step size and spectral resolution

To ensure that all features (frequencies) in $R(\lambda)$ are adequately resolved, the monochromator step size, expressed in the optical frequency domain ($\Delta\nu$) must be a factor of two smaller than the "oscillation frequency" corresponding to the maximum $\delta\tau$ measured (Nyquist condition):

$$\delta\tau_{\max} = 1/(2 \cdot \Delta\nu) \quad (5-30)$$

If from the Fourier transform, it is evident that significant energy is present near to $\delta\tau_{\max}$ (i.e., that $R(\lambda)$ appears to be "aliased"), it will be necessary to reduce the step size $\Delta\nu$ (if possible) and repeat the measurement.

The monochromator spectral linewidth (resolution) expressed in optical frequency units is generally equal to or smaller than the smallest $\Delta\nu$ value to be used (corresponding to the largest $\delta\tau$ value to be measured).

For example, for $\delta\tau_{\max} = 1.34$ ps, a monochromator linewidth of 3 nm at 1550 nm ($\Delta\nu = 374$ GHz) is typical.

5.1.4.4.3 Cosine Fourier analysis

This analysis is based on the observation that the cosine Fourier transform of the spectrum emitted from the analyser is the fringe pattern of the interferogram. The difference between fringe patterns generated by the analyser being set at two orthogonal settings is the cross-correlation function. For an infinite spectrum into the analyser, the autocorrelation function would have zero width. In practice, the finite source spectrum in the optical frequency domain (finite linewidth) acts as a windowing function which produces a non-zero autocorrelation function width in the time domain.

The analysis of the squared cross-correlation and autocorrelation functions found in the GINTY analysis of 5.1.3 shows that the difference in squared RMS widths of these functions is proportional to the square of the spectrally weighted RMS (by squared power) of the DGD values. (See Equation 5-22.)

The result is independent of the spectral shape which means that the details of the windowing function are fully taken into account. It is also independent of the degree of mode coupling, which means that no changes in algorithm are needed to treat the different regimes.

The result is limited by the spectral width and optical frequency increment that is measured. As the PMD increases, the frequency increment must be decreased. At some limit it would be more practical to use the interferometric method (GINTY).

The analysis reports the PMD_{RMS} metric. If random mode coupling is found, the result can be converted to PMD_{AVG} using Equation 3-3.

5.1.4.4.3.1 Overview

The measurement of the powers emitted from the analyser set at two orthogonal settings is required. The ratio, R , associated with Equation 5-24 is modified to:

$$R(\nu) = \frac{P_A(\nu) - P_B(\nu)}{P_A(\nu) + P_B(\nu)} \quad (5-31)$$

where $\nu = c/\lambda$ is the optical frequency (THz).

If a polarimeter is used, the three normalized output Stokes vector elements are equivalent to three independent normalized ratios equivalent to that represented by Equation 5-31. Each Stokes vector element is the difference in powers between orthogonal analyser settings. The three elements are different in that the base settings are also orthogonal.

The data are multiplied by a windowing function, $W(\nu)$, that goes to zero smoothly at the edges. Both $R(\nu)W(\nu)$ and $W(\nu)$ are put into arrays with zero padding at lower, unmeasured frequencies. Fast Cosine Fourier Transforms (FCFT) are applied to each array to obtain the time domain fringe envelopes, $r(t)w(t)$ and $w(t)$. These are squared to obtain the squared cross-correlation and autocorrelation envelopes, E_x^2 and E_0^2 , respectively. When multiple ratio functions (N) are available from different combinations of input polarizer setting and base analyser settings (or different Stokes output vector elements), using for instance input/output SOP scrambling, form the mean square envelopes as:

$$\bar{E}_x^2 = \frac{1}{N} \sum_i E_{xi}^2 \quad \bar{E}_0^2 = \frac{1}{N} \sum_i E_{0i}^2 \quad (5-32)$$

Using the RMS calculation of Appendix I.2, calculate the RMS widths, σ_x and σ_0 of these two functions. The PMD_{RMS} value is calculated as:

$$PMD_{RMS} = \left[\frac{3}{2} (\sigma_x^2 - \sigma_0^2) \right]^{1/2} \quad (5-33)$$

It is related to the spectrally weighted (by squared window value) RMS of the DGDs as:

$$\langle PMD_{RMS} \rangle = \frac{\int \Delta\tau^2(\nu) W^2(\nu) d\nu}{\int W^2(\nu) d\nu} \quad (5-34)$$

The expected value operator is with respect to random input/output SOPs.

5.1.4.4.3.2 Details

This clause explains some of the details with respect to the measured frequency window, the frequency increment, $\Delta\nu$, frequency shifting, and the result of the FCFT. An example of a FCFT algorithm may be found in *Numerical Recipes in C*, by W. Press, W. Vetterling, S. Teukolsky and B. Flannery, Cambridge University Press.

The data must be available in uniform frequency increments. The number of data points, including zero pad values, must be $1+2^k$, with k an integer.

If the n_m data measured data points are not taken in uniform frequency increments, they may be fitted to a polynomial such as a spline for interpolation. A cubic spline with $n_m - 3$ uniform segments will fit all the data perfectly and allow interpolation.

Given that the measured data are bounded by $v_{\min M}$ and $v_{\max M}$ and the fact that the minimum optical frequency is well above zero, the application of frequency shifting can be used to reduce the size of the arrays that are processed. The boundaries of the frequencies used in the calculation array can be selected by any choice of n such that:

$$v_{\max} \frac{n-1}{n} = v_{\min} \leq v_{\min M}, v_{\max} = v_{\max M}, \text{ and } n \text{ is a positive integer.} \quad (5-35)$$

The frequency values less than the measured frequency are filled with zeros.

Following the FCFT, the array will contain the time domain fringe pattern from times of 0 to $t_{\max} = \Delta t 2^k$, where the time increment, Δt , is given as:

$$\Delta t = \frac{n}{2v_{\max}} = \frac{1}{2(v_{\max} - v_{\min})} \quad (5-36)$$

The fringe pattern that would be obtained from interferometry extends to negative time values as well as positive time values. The value at a given negative time is equal to the value at the positive time. The function is even and symmetric about zero. This can lead to simplifying the calculation of RMS since time zero is known.

The selection of the frequency shift should be done keeping in mind that the RMS width calculation needs some time domain values that are less than the minimum PMD_{RMS} that is measurable.

The frequency increment, Δv , is also related to the number of points sampled, the frequency shift, and the maximum PMD_{RMS} that is to be measured. It is given as the following, along with the constraint as:

$$\Delta v = \frac{v_{\max} - v_{\min}}{2^k} \leq \frac{1}{24PMD_{RMS-\max}} \quad (5-37)$$

The constraint in Equation 5-37 is consistent with Equation 5-26. The spectral width of the filtered source should be half of this value. When the actual scan is done in equal wavelength increments, the wavelength increment at the lower end of the range should be consistent with the constraint of Equation 5-37.

The windowing function, $W(v)$, can technically be any function, including a square function. The function that is chosen should be one that minimizes the value of σ_0 . Functions that do this proceed to zero at the edges in a continuous way and should also have the first derivative proceed to zero at the edges. This will minimize the ringing that can increase σ_0 .

5.1.4.4.3.3 Examples

Table 1 shows a sample calculation spreadsheet. The wavelength extrema and k are entered. For each of several possible frequency shift values, n , the other parameters are calculated. PMD_{\min} is calculated as $3\Delta t$. The effective shift in terms of $\Delta\lambda$ at the lower wavelength limit is also presented. Clearly there are tradeoffs, depending on the range of PMD_{RMS} values that are to be measured. In general, the broader the wavelength range and the smaller the frequency increment, the better.

Table 1/G.650.2 – Cosine transform calculations

c	299792.5	nm/ps				
k	11					
npt	2048					
wavelengths (nm)		frequencies (THz)				
max	1700	230.6096				
min	1300	176.3485				
Frequency shift						
n	freqmincalc (THz)	del-t (ps)	delfreq (THz)	minPMD (ps)	maxPMD (ps)	wave increment (nm)
1	0	0.002168	0.112602	0.006504	0.370034	0.635076
2	115.3048077	0.004336	0.225205	0.013009	0.185017	1.270772
3	153.7397436	0.006504	0.337807	0.019513	0.123345	1.90709
4	172.9572115	0.008673	0.450409	0.026018	0.092508	2.544031
5	184.4876923	0.010841	0.563012	0.032522	0.074007	3.181596
6	192.1746795	0.013009	0.675614	0.039027	0.061672	3.819785
7	197.6653846	0.015177	0.788216	0.045531	0.052862	4.458599
8	201.7834135	0.017345	0.900819	0.052036	0.046254	5.098039

The following illustrates the results for what might be obtained from a fibre with $PMD_{RMS} = 0.2$ ps. The mean cross-correlation and mean autocorrelation envelopes from a single scan using a windowing function that is Gaussian with a standard deviation of 23 nm are shown in Figure 17. The result is from a simulation of a fibre with ideal random mode coupling. The measured result for this simulation was 0.185 ps.

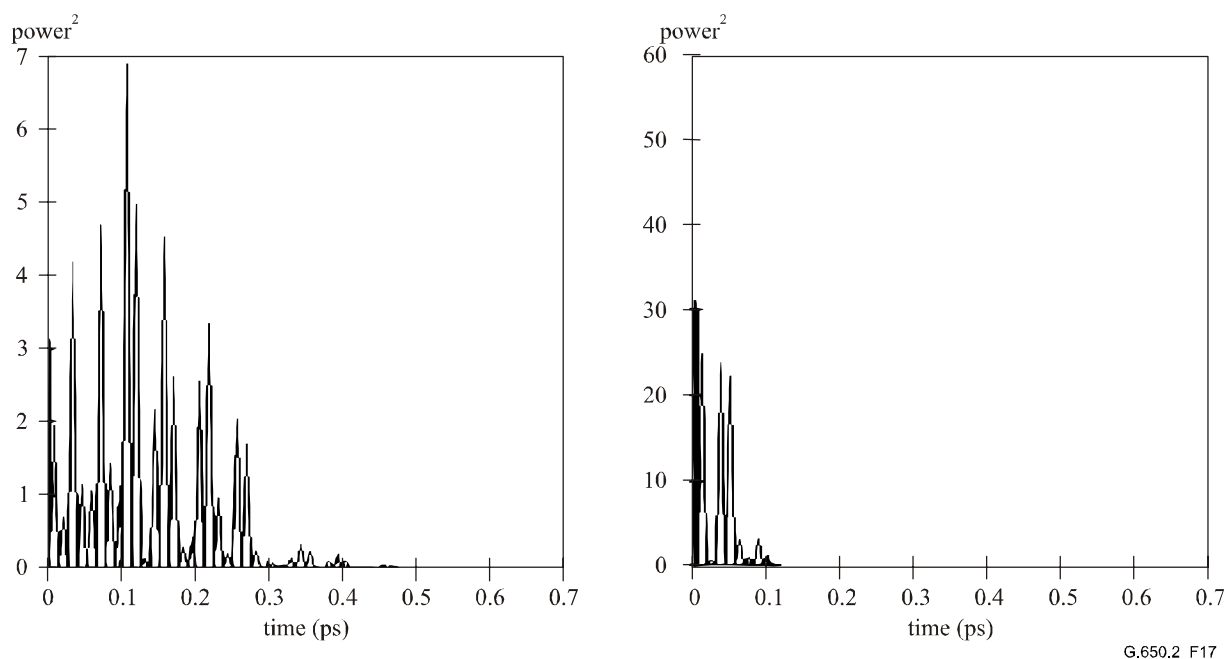


Figure 17/G.650.2 – Cross-Correlation and autocorrelation functions

5.1.4.5 Presentation of the results

- a) Identification of the fibre and/or cable measured.
- b) Test length.
- c) Polarization mode dispersion (typically in picoseconds). If the degree of mode coupling is known, the PMD coefficient may be given in ps/km (negligible mode coupling) or ps/km^{1/2} (strong mode coupling).
- d) The wavelength range over which the measurement was performed, and the wavelength or frequency step size.
- e) The physical configuration of the fibre or cable sample.
- f) Mode coupling type, e.g., deterministic, semi-random or random.
- g) When an average PMD has been obtained from repeated measurements of the sample, record the number of measurements performed.

5.2 Test methods for non-linear attributes

(Under study).

Appendix I

Determination of PMD delay from an interferogram

This appendix presents two methods for the determination of the RMS width from fringe envelopes. These methods are mainly used for the interferometric method of measuring PMD. Clause I.1 is for an envelope with the autocorrelation peak present and is suitable for the TINTY analysis. Clause I.2 is for envelopes without this peak and is suitable for the GINTY analysis.

I.1 RMS calculation for TINTY

Figure I.1 shows a fringe envelope with an autocorrelation peak in the centre.

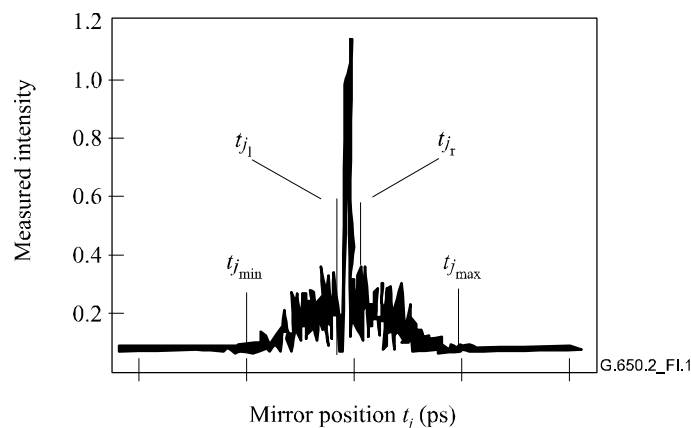


Figure I.1/G.650.2 – Parameters for interferogram analysis

Let \tilde{I}_j denote the measured intensity of the fringe envelope at increasing positions t_j , $j = 1 \dots N$, with $[t_j] = \text{ps}$.

Step 1 – Computation of the zero intensity \tilde{I}_0 and the noise amplitude Na

Definition: $N_5 = \text{round}(5 N/100)$

$$\tilde{I}_0 = \frac{\sum_{j=1}^{N_5} (\tilde{I}_j + \tilde{I}_{N-j})}{2N_5} \quad (\text{I-1})$$

$$X_2 = \frac{\sum_{j=1}^{N_5} (\tilde{I}_j^2 + \tilde{I}_{N-j}^2)}{2N_5} \quad (\text{I-2})$$

$$Na = \sqrt{X_2 - I_0^2} \quad (\text{I-3})$$

Step 2 – Definition of the shifted intensity I_j

$$I_j := \tilde{I}_j - \tilde{I}_0 \text{ if } \tilde{I}_j - \tilde{I}_0 > 4Na \quad (\text{I-4})$$

$$I_j := 0 \text{ if } \tilde{I}_j - \tilde{I}_0 \leq 4Na \quad (\text{I-5})$$

Step 3 – Computation of the centre C of the interferogram

$$C = \frac{\sum_{j=1}^N t_j I_j}{\sum_{j=1}^N I_j} \quad (\text{I-6})$$

Step 4 – Removal of the central autocorrelation peak

Definition: $j_l :=$ the largest index j such that $C - t_j > \tau_c$ (I-7)

$j_r :=$ the smallest index j such that $t_j - C > \tau_c$ (I-8)

where τ_c is the source coherence time.

NOTE 1 – For cross-correlation interferograms, the following definition shall be applied:

$$j_r := j_l + 1 \quad (\text{I-9})$$

Step 5 – Computation of the second moment S of the interferogram

$$S = \frac{1}{2} \left\{ \sqrt{\frac{\sum_{j=1}^{j_l} (t_j - C)^2 I_j}{\sum_{j=1}^{j_l} I_j}} + \sqrt{\frac{\sum_{j=j_r}^N (t_j - C)^2 I_j}{\sum_{j=j_r}^N I_j}} \right\} \quad (\text{I-10})$$

Step 6 – Truncate the interferogram

Set j_{\min} to the largest index j such that $C - t_j > 2S$ (I-11)

Set j_{\max} to the smallest index j such that $t_j - C > 2S$ (I-12)

Step 7 – Computation of the second moment σ_ε of the truncated interferogram

$$\sigma_\varepsilon = \frac{1}{2} \left\{ \sqrt{\frac{\sum_{j=j_{\min}}^{j_l} (t_j - C)^2 I_j}{\sum_{j=j_{\min}}^{j_l} I_j}} + \sqrt{\frac{\sum_{j=j_r}^{j_{\max}} (t_j - C)^2 I_j}{\sum_{j=j_r}^{j_{\max}} I_j}} \right\} \quad (\text{I-13})$$

Step 8 – Computation of the σ of the Gaussian $e^{-\frac{(t-C)^2}{2\sigma^2}}$ such that:

$$\sigma_\varepsilon = \frac{1}{2} \left\{ \sqrt{\frac{\int_{t_{j_{\min}}}^{t_{j_l}} (t-C)^2 e^{-\frac{(t-C)^2}{2\sigma^2}} dt}{\int_{t_{j_{\min}}}^{t_{j_l}} e^{-\frac{(t-C)^2}{2\sigma^2}} dt}} + \sqrt{\frac{\int_{t_{j_r}}^{t_{j_{\max}}} (t-C)^2 e^{-\frac{(t-C)^2}{2\sigma^2}} dt}{\int_{t_{j_r}}^{t_{j_{\max}}} e^{-\frac{(t-C)^2}{2\sigma^2}} dt}} \right\} \quad (\text{I-14})$$

Step 9 – Determination of $\text{PMD}_{\text{RMS}} <\Delta\tau^2>^{1/2}$

$$\text{PMD}_{\text{RMS}} = <\Delta\tau^2>^{1/2} = \sqrt{\frac{3}{4}} \sigma \quad (\text{I-15})$$

NOTE 2 – For appropriately measured interferograms, it can be shown that $\frac{\sigma_\varepsilon}{\sigma} \approx \sqrt{\frac{3}{4}}$

I.2 RMS calculation for GINTY

The following algorithm results in a robust RMS width for either the composite square cross-correlation or autocorrelation envelopes using Method D (GINTY).

The algorithm is iterative. For a given iteration, the full data array is divided into two sets: The central portion, M, containing the signal and the tails, T, which contain noise. Each iteration results in different definitions for these sets. The result converges when either the computed RMS width ceases to vary or when the set definitions stabilize. For an iteration, the number of data points in each set are denoted as N_M and N_T .

Let \tilde{I}_j denote the measured intensity of the envelope at increasing positions t_j (ps), (ps), $j = 1 \dots N$.

The initial definition of the set T is the first and last 5% of the whole array.

Step 1 – Computation of the zero \tilde{I}_0

$$\tilde{I}_0 = \sum_{j \in T} \tilde{I}_j / N_T \quad (\text{I-16})$$

Step 2 – Definition of the shifted intensity I_j

$$I_j = \tilde{I}_j - \tilde{I}_0 \quad \text{all } N \quad (\text{I-17})$$

Step 3 – Computation of the centre C of the interferogram

$$C = \frac{\sum_{j \in M} t_j I_j}{\sum_{j \in M} I_j} \quad (\text{I-18})$$

Step 4 – Computation of the RMS width σ of the squared envelope

$$\sigma^2 = \frac{\sum_{j \in M} (t_j - C)^2 I_j}{\sum_{j \in M} I_j} \quad (\text{I-19})$$

Step 5 – Redefine the sets

Define M as the set of points for which $C - 4\sigma \leq t_j \leq C + 4\sigma$

Define T as the rest of the points.

Step 6 – Repeat steps 1 to 5 until the results converge

$$\frac{\sigma_\varepsilon}{\sigma} \approx \sqrt{\frac{3}{4}}$$

Appendix II

Non-linear attributes

II.1 Background

Non-linear interactions between the signal and the silica fibre transmission medium begin to appear as optical signal powers and are increased to achieve longer span lengths at high bit rates. Consequently, non-linear fibre behaviour has emerged as an important consideration, both in high capacity systems and in long unregenerated routes. These non-linearities can be generally categorized as either scattering effects (stimulated Brillouin scattering and stimulated Raman scattering) or effects related to the Kerr effect, that is, the intensity dependence of the refractive index (self-phase modulation, cross-phase modulation, modulation instability, soliton formation and four wave mixing). A variety of parameters influence the severity of these non-linear effects, including fibre dispersion characteristics, the effective area of the fibre, the number of spacing of channels in multiple channel systems, overall unregenerated system length, the degree of longitudinal uniformity of the fibre characteristics, as well as signal intensity and source linewidth.

II.2 Effective area (A_{eff})

Effective area is a parameter that is closely related to optical fibre non-linearities that will affect the transmission quality of the optical fibre systems, especially in long-haul optically amplified systems.

Effective area A_{eff} is defined as follows:

$$A_{\text{eff}} = \frac{2\pi \left[\int_0^{\infty} I(r) r dr \right]}{\int_0^{\infty} I(r)^2 r dr} \quad (\text{II-1})$$

where $I(r)$ is the field intensity distribution of the fundamental mode of the fibre at radius r . The integration of Equation II-1 is carried out over the entire cross-sectional area of the fibre. For example, if we make a Gaussian approximation such that:

$$I(r) = \exp(-2r^2 / W^2) \quad (\text{II-2})$$

where $2w$ is the Mode Field Diameter (MFD), then Equation II-1 can be analytically integrated and gives:

$$A_{\text{eff}} = \pi w^2 \quad (\text{II-3})$$

The Gaussian approximation is accurate for G.652 [1] and G.654 [3] step-index fibres near the LP_{11} cut-off, but for G.652 and G.654 fibres at much longer wavelengths, and in the case of G.653 [2] dispersion shifted fibres, A_{eff} cannot be accurately estimated from Equation II-3.

A more general but empirical relationship between A_{eff} and w is¹:

$$A_{\text{eff}} = k\pi w^2 \quad (\text{II-4})$$

where k is a correction factor.

II.3 Correction factor k

In the experiment, the Mode Field Diameter (MFD) was measured by the variable aperture test method. From the Far-Field Pattern (FFP) of the output optical power $P(r)$, it was then possible to calculate the Near-Field Pattern (NFP) using an inverse Hankel transformation. A_{eff} is then derived from the NFP by using Equation II-1.

The correction factor k in Equation II-4 depends on the wavelength and on fibre parameters such as refractive index profiles, MFD and zero-dispersion wavelength.

Figure II.1 shows examples of measured wavelength dependence of MFD and A_{eff} for G.652 and G.653 fibres in the 1200-1600 nm wavelength regions. Figure II.2 gives examples of calculated and measured wavelength dependence of MFD, A_{eff} , and the correction factor k for G.652, G.653, and G.654 fibres in this same wavelength region.

The ranges of the correction factor k for these examples are summarized in Table II.1.

For other fibre designs that may be developed for optical submarine and WDM applications, the relationship of A_{eff} to w may vary, and should be determined using Equation II-1.

Figure II.3 shows the wavelength dependence of A_{eff} for G.653 (DSF) and G.655 (NZ-DSF) fibres in the 1520-1580 nm wavelength regions for WDM applications.

The average k values and standard deviation were found to be around $0.953 \pm .005$ for the G.653 fibres, and $1.09 \pm .070$ for the G.655 fibres.

¹ NAMIHIRA (Y.): Relationship between non-linear effective area and mode field diameter for dispersion shifted fibres, *Electron. Lett.*, Vol. 30, No. 3, pp. 262-263, 1994.

Table II.1/G.650.2 – Summary of correction factor k of A_{eff} and MFD ($= 2W$) for G.652, G.653 and G.654 fibres based on the examples in Figure II.2

Wavelength λ	~ 1310 nm	~ 1550 nm
Fibre types		
ITU-T Rec. G.652	0.970 ~ 0.980 (Note)	0.960 ~ 0.970
ITU-T Rec. G.654	...	0.975 ~ 0.985 (Note)
ITU-T Rec. G.653	0.940 ~ 0.950	0.950 ~ 0.960 (Note)

NOTE – Optimum wavelength region.

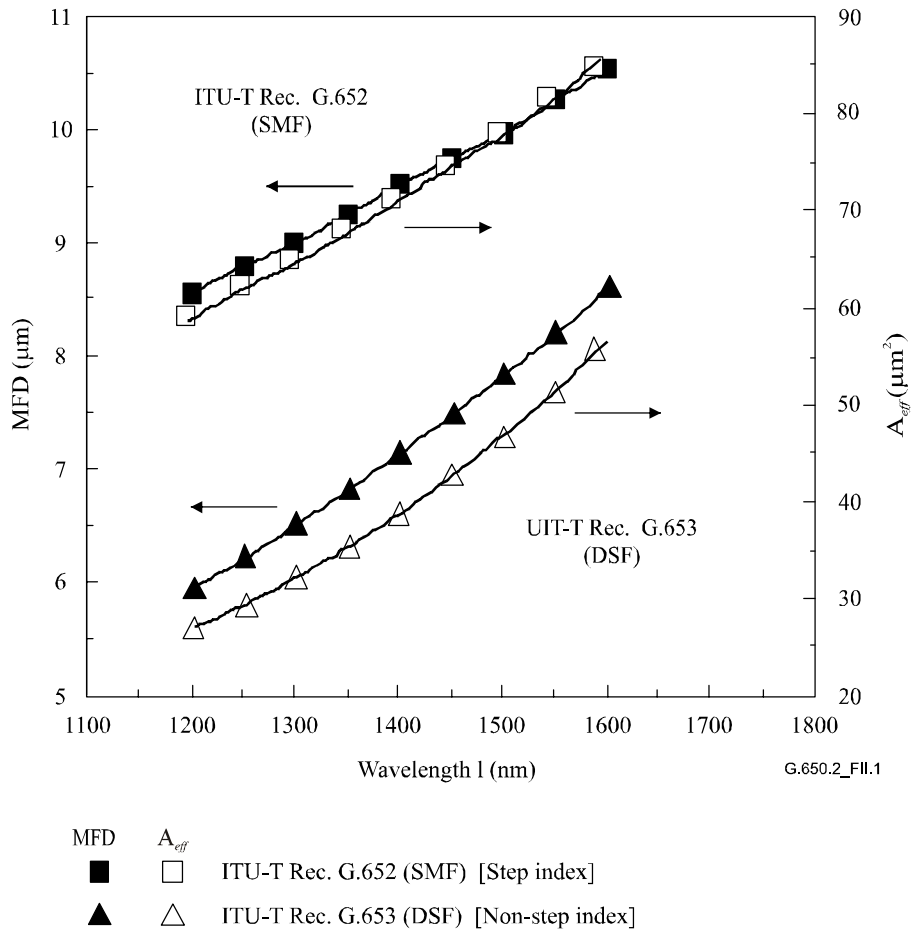


Figure II.1/G.650.2 – Example of measured wavelength dependence of A_{eff} and MFD ($= 2W$) of G.652 and G.653 fibres

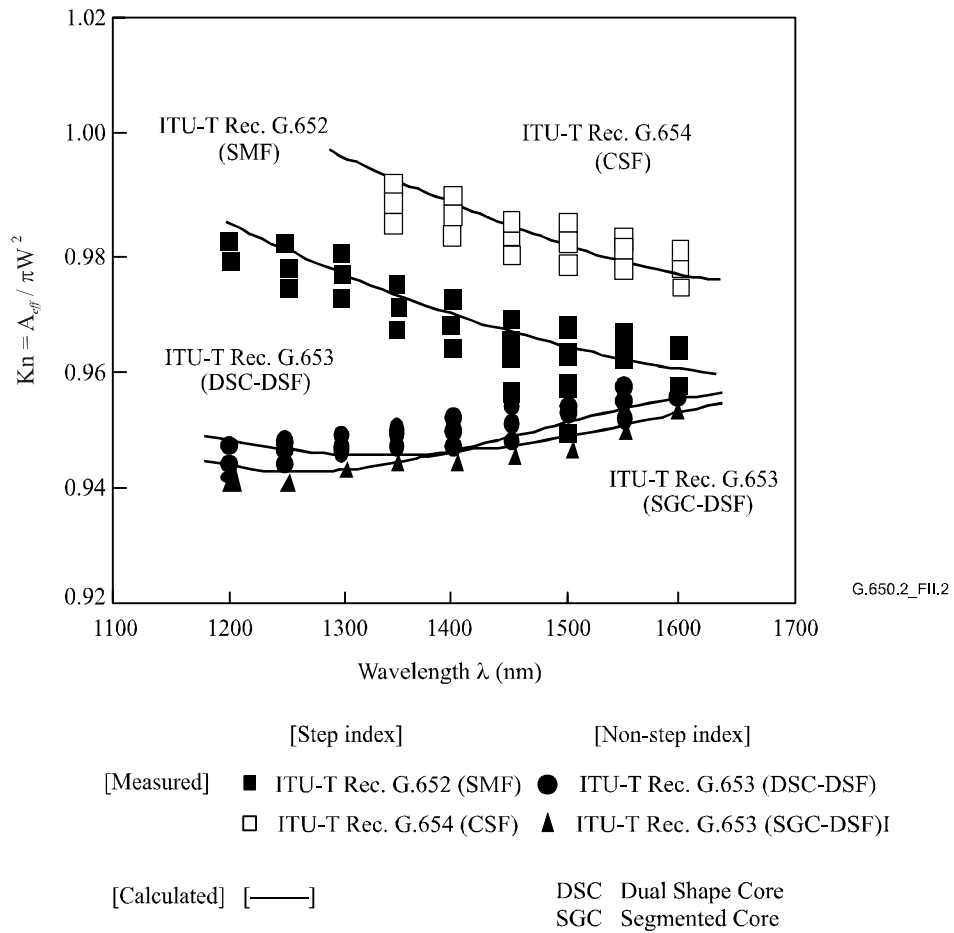


Figure II.2/G.650.2 – Example of calculated and measured wavelength dependence of correction factor k for G.652, G.653 and G.654 fibres

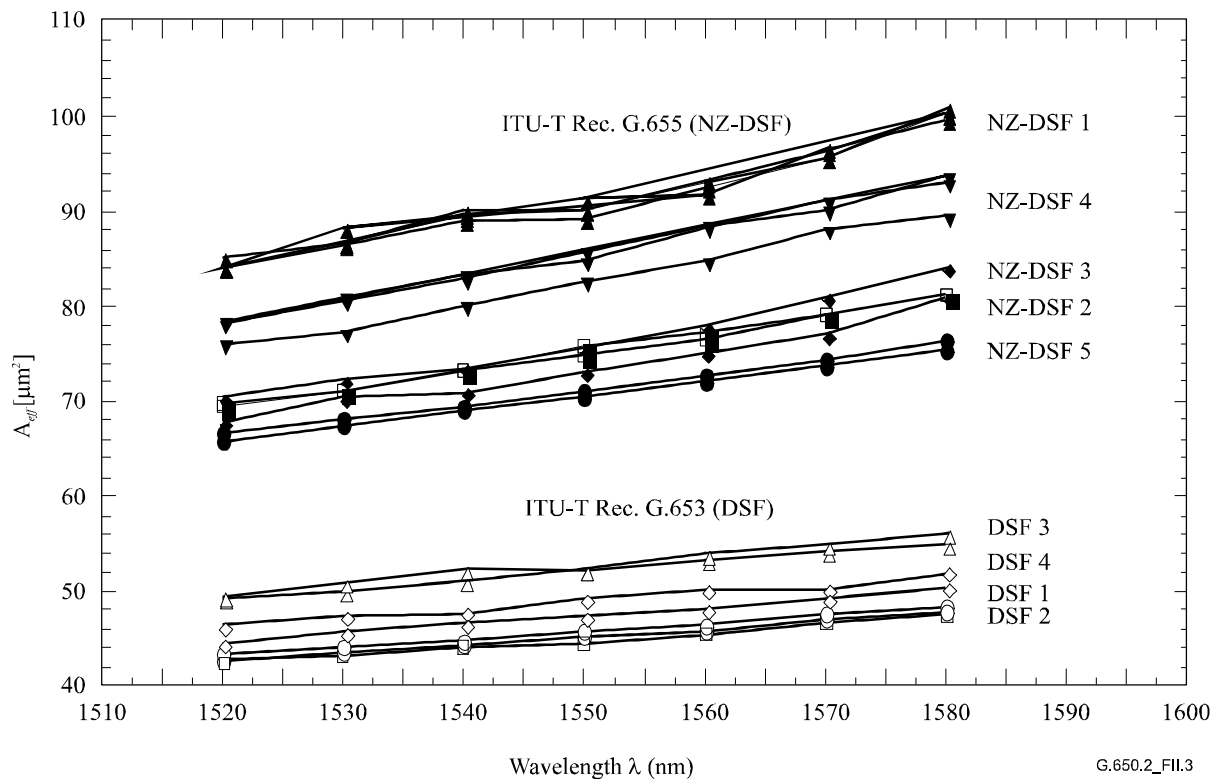


Figure II.3/G.650.2 – Example of measured λ dependence of A_{eff} for G.653 and G.655 fibres

II.4 Non-linear coefficient (n_2/A_{eff})

For particularly intense fields, the refractive index of optical fibres is dependent on optical intensity inside the fibres, and can be expressed as:

$$n = n_0 + n_2 I \quad (\text{II-5})$$

where n is the refractive index, n_0 the linear part of the refractive index, n_2 the non-linear refractive index and I the optical intensity inside the fibres.

The non-linear coefficient is defined as n_2/A_{eff} . This coefficient plays an important role in evaluating the system performance degradation due to non-linearities when high power density systems are used.

Methods for measuring the non-linear coefficient are under study.

II.5 Stimulated Brillouin scattering

The SBS threshold defined in this clause has been called into question for certain transmissions applications. The study of alternative definitions has begun, but is not complete. A corrigendum with modifications to the following clause is anticipated.

II.5.1 Description of the effect

In an intensity-modulated system using a source with a narrow linewidth, significant optical power is transferred from the forward-propagating signal to a backward-propagating signal when the Stimulated Brillouin Scattering (SBS) threshold is exceeded. In SBS, the forward-propagating light is scattered from acoustic phonons. Phase matching (or momentum conservation) dictates that the scattered light preferentially travels in the backward direction. The scattered light is downshifted or Brillouin-shifted by approximately 11 GHz at 1550 nm.

II.5.2 SBS threshold estimation for single-mode fibres

II.5.2.1 SBS threshold

In general, the SBS threshold is expressed as:

$$P_{th} = 21 \frac{KA_{eff}}{gL_{eff}} \frac{\Delta\nu_p + \Delta\nu_B}{\Delta\nu_B} \quad (\text{II-6})$$

where a Lorentzian pump and Brillouin linewidth is assumed, and g denotes the Brillouin gain coefficient (units of length/power) and A_{eff} the effective area. K is a constant ($1 \leq K \leq 2$) determined by the degree of freedom of the polarization state. $\Delta\nu_B$ and $\Delta\nu_p$ represent the Brillouin bandwidth and the linewidth of the pump light (MHz) respectively. L_{eff} denotes the effective length defined as:

$$L_{eff} = \frac{1 - \exp(-\alpha L)}{\alpha} \quad (\text{II-7})$$

where α is the attenuation coefficient and L is fibre length.

The SBS threshold, P_{th} , depends on the linewidth, $\Delta\nu_p$, of the pump light. When $\frac{\Delta\nu_p}{\Delta\nu_B} \ll 1$, P_{th} attains its minimum value, which defines the maximum steady state input power, P_m , in the absence of either a broader pump linewidth or other modulation schemes. The maximum input power can be written as:

$$P_m = 21 \frac{KA_{eff}}{gL_{eff}} \quad (\text{II-8})$$

NOTE 1 – The actual maximum input power of a transmission system can be increased by various modulation schemes that have been reported in the literature.

NOTE 2 – Both P_{th} and P_m require an estimate of the gain coefficient, g , which must be determined experimentally and, optionally, characterized as a function of mode field diameter for a given fibre design.

II.5.2.2 Experimental set-up for SBS threshold

Figure II.4 shows a set-up to measure SBS threshold. The 1.32 μm pump is a LD pumped Nd:YAG single frequency laser with linewidth of about 5 kHz. The 1.55 μm pump is a single-mode DFB LD with a 200 kHz linewidth. The CW light from the DFB source was amplified by an Er-doped fibre amplifier. The linewidths of the pump lights are considered to be negligible compared with $\Delta\nu_B$ (20 to 100 MHz). The CW pump light is launched into the test fibre through a fibre coupler with a branching ratio of 1.9. The input, transmitted and backscattered light powers are monitored by power meters.

Figure II.5 shows an example of the transmitted and backscattered power at 1.32 μm as a function of input power for a G.654 [3] fibre. The transmitted power stops increasing and the backscattered power rapidly increases as the input power reaches a certain power level. The SBS threshold is defined as the input pump power which produces a backscattered Stokes power equal to the transmitted pump power (see Figure II.5). Table II.2 summarizes the fibre parameters and SBS thresholds for various fibre types.

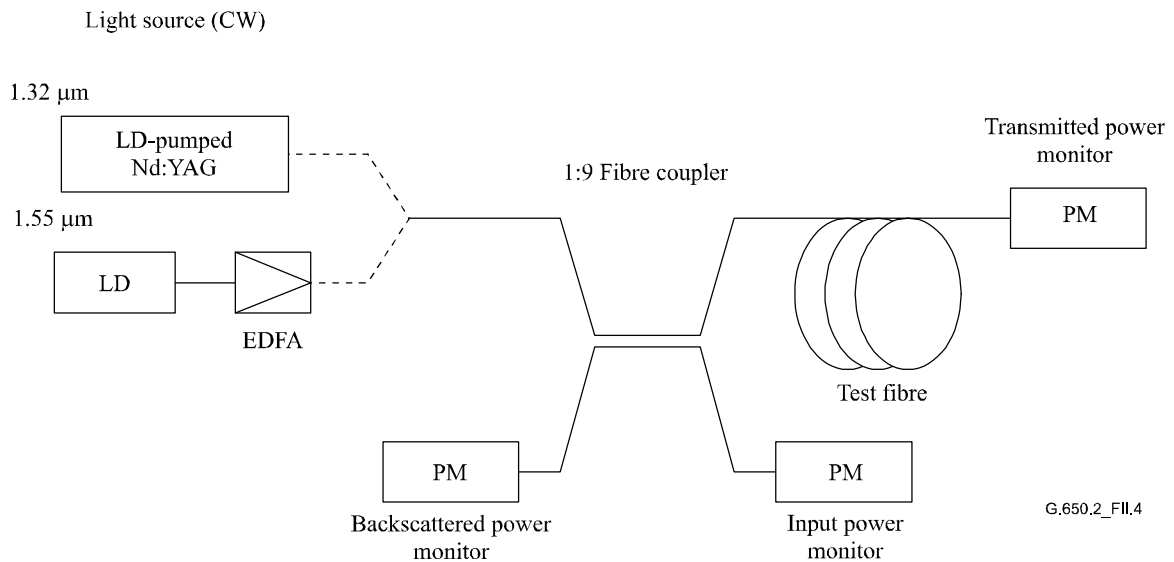


Figure II.4/G.650.2 – Experimental set-up

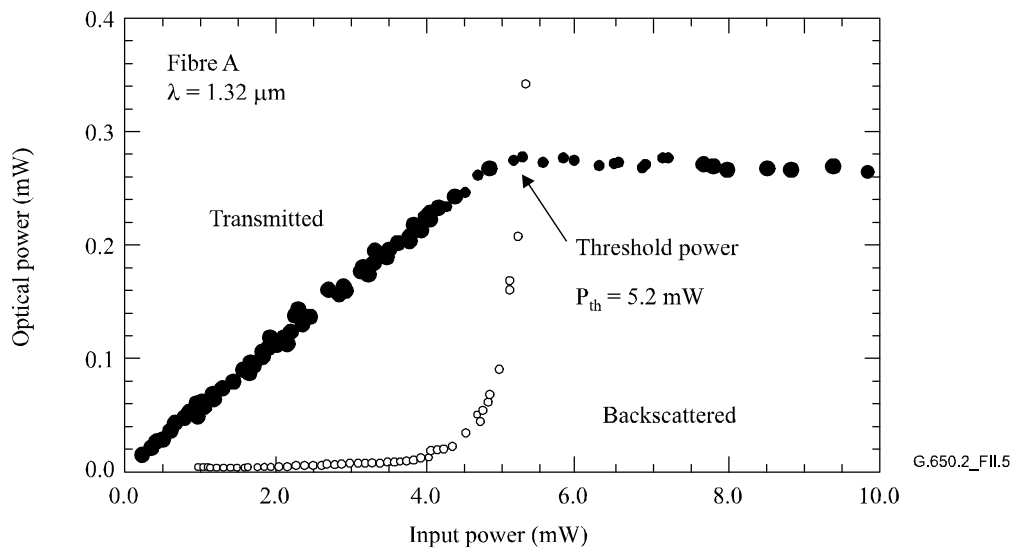


Figure II.5/G.650.2 – Transmitted and backscattered power as a function of input power

Threshold powers in Table II.2 are only valid for the test fibres under the described test conditions. In the normal implementation of transmission systems, significantly higher values may apply.

Table II.2/G.650.2 – Test fibre parameters

Fibre		A	B	C	D	E	F	G
Fibre type		ITU-T Rec. G.654	ITU-T Rec. G.652	ITU-T Rec. G.653				
Length L (km)		41.3	32.0	20.2	25.2	24.1	21.6	30.0
Loss (dB/km)	1320 nm	0.302	0.322	0.360	0.360	0.360	0.362	0.364
	1550 nm	0.172	0.194	0.200	0.200	0.200	0.200	0.209
MFD (µm)	1320 nm	9.1	9.8	6.3	6.5	6.3	6.7	6.2
	1550 nm	10.1	10.9	7.8	8.1	7.8	8.3	7.6
Brillouin frequency shift change (MHz)		1	1.5	1.5	–	–	–	6.0
Threshold power (mW)	1320 nm	5.2	6.4	3.3	3.4	2.9	3.6	4.1
	1550 nm	4.2	5.3	3.9	3.7	3.3	4.4	4.0

II.5.2.3 SBS threshold estimation

Figure II.6 shows the relationship between SBS threshold and $A_{\text{eff}}/L_{\text{eff}}$ for the test fibres. It shows that the SBS threshold is linearly dependent on $A_{\text{eff}}/L_{\text{eff}}$. The SBS threshold can be estimated as the following equation:

$$P_{th} = 0.11 \left[\frac{A_{\text{eff}}}{L_{\text{eff}}} \right] \quad (\text{II-9})$$

where A_{eff} is in μm^2 , L_{eff} in km and P_{th} in mW.

Equation II-9 can be rewritten by using fibre length L , mode field diameter $2W$ and attenuation coefficient α as:

$$P_{th} = 0.11 \left[k\pi \left(\frac{2W}{2} \right)^2 \frac{\alpha}{1 - \exp(-\alpha L)} \right] \quad (\text{II-10})$$

Here, k is a correction factor that relates mode field diameter to A_{eff} for a particular fibre design and wavelength.

NOTE – If the Brillouin frequency shift changes by more than several MHz along the fibre, P_{th} will be larger than the value given by Equation II-9.

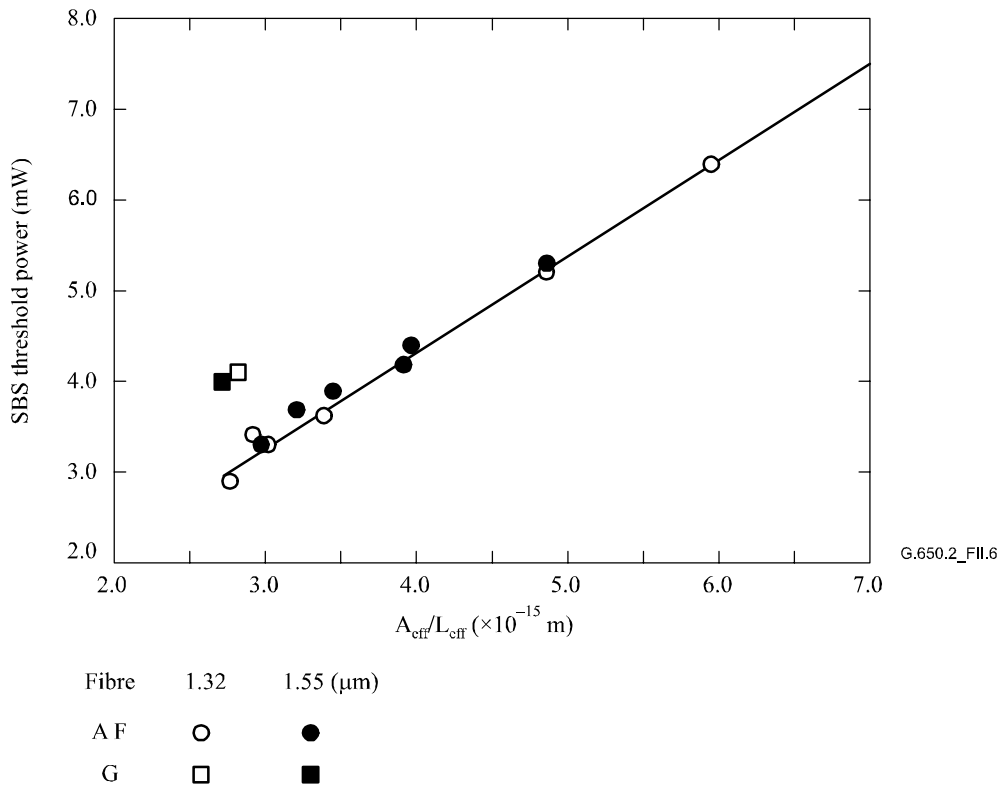


Figure II.6/G.650.2 – Relationship between SBS threshold and $A_{\text{eff}}/L_{\text{eff}}$

II.6 Other effects

For a description of other optical non-linear effects (four-wave mixing, modulation instability, self-phase modulation, cross-phase modulation, solitons and stimulated Raman scattering), see Appendix II/G.663.

Appendix III

Test methods for effective area (A_{eff})

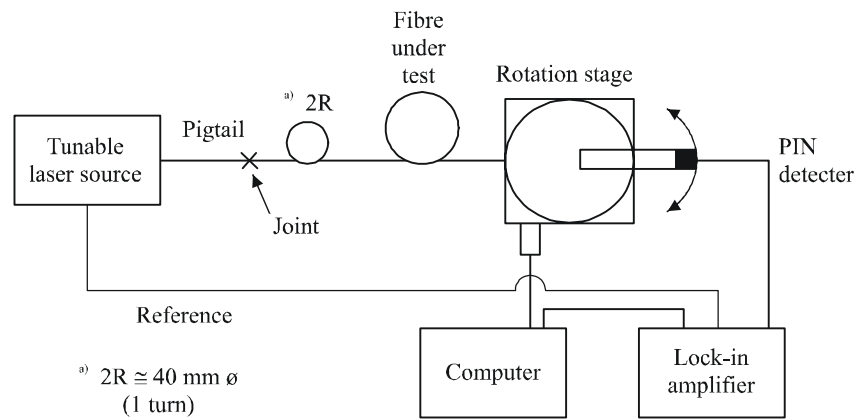
III.1 The far-field scan (FFS) technique

III.1.1 General

The effective area (A_{eff}) of single mode optical fibres is determined by the far-field scan (FFS) technique.

III.1.2 Test apparatus

A schematic diagram of the test set-up for far-field scan (FFS) is shown in Figure III.1.



G.650.2_FIII.1

Figure III.1/G.650.2 – Typical arrangement of far-field scan (FFS) set-up

- III.1.2.1 Light source** (as in 5.1.1.2.1/G.650.1)
- III.1.2.2 Modulation** (as in 5.1.1.2.2/G.650.1)
- III.1.2.3 Launching conditions** (as in 5.1.1.2.3/G.650.1)
- III.1.2.4 Cladding mode stripper** (as in 5.1.1.2.4/G.650.1)
- III.1.3.5 Specimen** (as in 5.1.1.2.5/G.650.1)
- III.1.2.6 Scan apparatus** (as in 5.1.1.2.6/G.650.1)
- III.1.2.7 Detector** (as in 5.1.1.2.7/G.650.1)
- III.1.2.8 Amplifier** (as in 5.1.1.2.8/G.650.1)
- III.1.2.9 Data acquisition** (as in 5.1.1.2.9/G.650.1)

III.1.3 Measurement procedure

The launch end of the fibre shall be aligned with the launch beam, and the output end of the fibre shall be aligned to the appropriate output device.

The effective area (A_{eff}) is computed from Equation III-1.

III.1.3.1 Equipment calibration

For equipment calibration, the magnification of the magnifying optics shall be measured by scanning the length of a specimen whose dimensions are already known with suitable accuracy. This magnification shall be recorded.

III.1.3.2 Calculations

III.1.3.2.1 Equations and figures for effective area (A_{eff}) calculation

1) *Fold the far-field radiation power data*

Let $P(\theta_i)$ be the measured power as a function of angular position, θ_i (radians) indexed by i . The folded power curve, $P_f(\theta_i)$, for $0 \leq \theta_i \leq \theta_{\text{max}}$ is:

$$P_f(\theta_i) = \frac{P(\theta_i) + P(-\theta_{-i})}{2} \quad \text{(III-1)}$$

2) *Compute the near-field intensity pattern*

Use an appropriate numerical integration method to compute the integrals of Equation III-1. Equation III-2 is an example. Any other integration method shall be at least as accurate.

Calculate the near-field values for a range of radii, r_j , values ranging from zero to a value large enough that the computed intensity at the maximum radius is less than 0.01% of the maximum intensity.

$$I(r_j) = \left[\sum_0^n P_f^{1/2}(\theta_1) J_0 \left(\frac{2\pi r_j \sin(\theta_i)}{\lambda} \right) \sin(2\theta_i) \Delta\theta \right]^2 \quad (\text{III-2})$$

where $\Delta\theta = \theta_1 - \theta_0$

3) *Compute the integrals of Equation III-2*

Use an appropriate numerical integration method to compute the integrals of Equation III-2. Equation III-3 is an example. Any other integration method shall be at least as accurate.

$$T = \left[\sum_0^m I(r_j) r_j \Delta r \right]^2 \quad (\text{III-3})$$

$$B = \sum_0^m I^2(r_j) r_j \Delta r \quad (\text{III-4})$$

where $\Delta r = r_1 - r_0$, and m is the number of positions measured.

4) *Complete the calculation*

$$A_{eff} = \frac{2\pi T}{B} \quad (\text{III-5})$$

An example measured far-field power data is shown in Figure III.2.

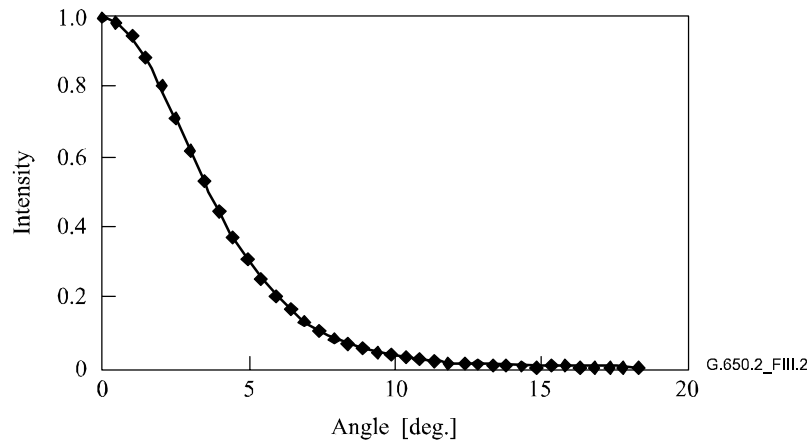


Figure III.2/G.650.2 – Example of measured FFP data

III.1.4 Presentation of the results

The following details shall be presented:

- a) Test set-up arrangement, dynamic range of the measurement system, processing algorithms, and a description of the aperture assembly used (including the NA).
- b) Launching conditions.
- c) Wavelength and spectral linewidth FWHM of the source.

- d) Fibre identification and length.
- e) Type of cladding mode stripper.
- f) Type and dimensions of the detector.
- g) Temperature of the sample and environmental conditions (when necessary).
- h) Indication of the accuracy and repeatability.
- i) Effective area (A_{eff}).
- j) Plot of $A_{eff}(\lambda)$ (if required).

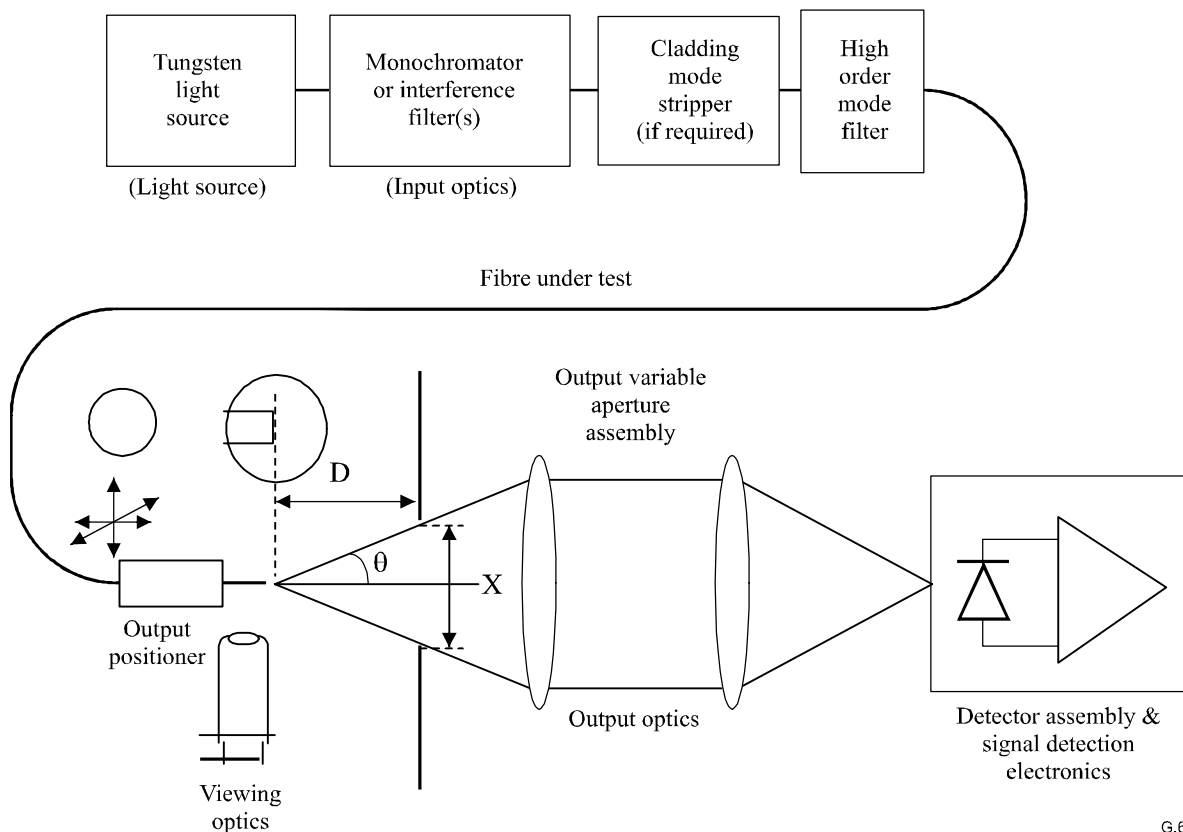
III.2 The variable aperture (VA) technique

III.2.1 General

The effective area (A_{eff}) of single-mode fibres is determined by the variable aperture in the far-field (VA) measurement technique.

III.2.2 Test apparatus

A schematic diagram of the test set-up for VA technique is shown in Figure III.3.



G.650.2_FIII.3

Figure III.3/G.650.2 – Typical arrangement of the variable aperture (VA) technique set-up

III.2.2.1 Light source (as in 5.1.1.2.1/G.650.1)

III.2.2.2 Modulation (as in 5.1.1.2.2/G.650.1)

III.2.2.3 Launching conditions (as in 5.1.1.2.3/G.650.1)

III.2.2.4 Cladding mode stripper (as in 5.1.1.2.4/G.650.1)

III.2.2.5 Specimen (as in 5.1.1.2.5/G.650.1)

III.2.2.6 Aperture apparatus

A mechanism containing at least twelve apparatus spanning the half-angle range of numerical apertures from 0.02 to 0.25 (0.4 for fibres covered by ITU-T Rec. G.653) should be used. Light transmitted by the aperture is collected and focused onto the detector.

NOTE – The NA of the collecting optics must be large enough not to affect the measurement results.

III.2.2.7 Output variable aperture assembly

A device consisting of round transmitting apertures of various sizes (such as an aperture wheel), shall be placed a distance D of at least $100 w^2 / \lambda$ from the fibre end, and is used to vary the power collected from the fibre output pattern. Typically 12 to 20 apertures are used and are located about 20-50 mm away from the fibre end. The maximum numerical aperture of the test set shall be = 0.40. Means of centering the apertures with respect to the pattern shall be employed to decrease sensitivity to fibre end-angle.

As part of equipment set-up (as shown in Figure III.4), carefully measure and record the longitudinal distance D between the fibre output end position and the aperture plane and the diameters X_i of each aperture. Determine the half-angle subtended by each aperture in the wheel and record these θ_i , ($i = 1$ to n in order of increasing aperture size) values for future calculation. These values are independent of test wavelength.

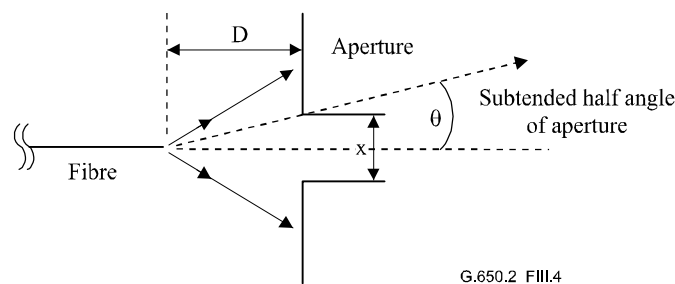


Figure III.4/G.650.2 – Aperture apparatus set-up

III.2.2.8 Detector (as in 5.1.1.2.7/G.650.1)

III.2.2.9 Amplifier (as in 5.1.1.2.8/G.650.1)

III.2.2.10 Data acquisition (as in 5.1.1.2.9/G.650.1)

III.2.3 Measurement procedure

The launch end of the fibre shall be aligned with the launch beam, and the output end of the fibre shall be aligned to the appropriate output device.

The effective area (A_{eff}) is computed from Equations III-6 to III-10.

III.2.3.1 Equipment calibration

For equipment calibration the magnification of the magnifying optics shall be measured by scanning the length of a specimen whose dimension are already known with suitable accuracy. This magnification shall be recorded.

III.2.3.2 Calculations

III.2.3.2.1 Equations and figures for effective area (A_{eff}) calculation

The variable aperture (VA) technique measures the total normalized power $f(\theta)$ passing through a given aperture as shown in Figure III.3 subtending a far-field angle θ at the fibre. These power

values are equivalent to an integration of the normalized far-field power distribution $F^2(\theta)$. This is represented by Equation III-6.

$$f(\theta) = \int_0^{\theta} F^2(\theta) \sin(\theta) d\theta \quad (\text{III-6})$$

A plot of normalized power transmitted through the apertures as a function of angle θ is shown in Figure III.5.

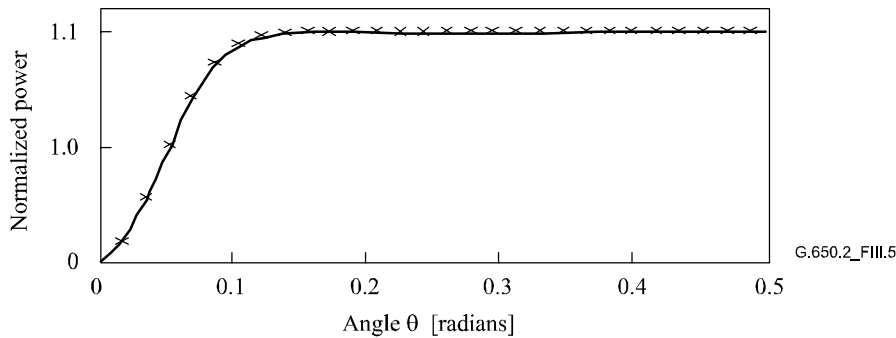


Figure III.5/G.650.2 – Plot of measured VA data

A quartic function is fitted to far-field aperture data, given by Equation III-7:

$$f(\theta) = A\theta^4 + B\theta^3 + C\theta^2 + D\theta^1 + E \quad (\text{III-7})$$

Effective area, A_{eff} , is calculated from the near-field power distribution $I(r)$ given as a function of radius r . To calculate this, one must first differentiate the integrated power data, $f(\theta)$, to give the far-field power distribution $F^2(\theta)$,

$$F^2(\theta) = \frac{df(\theta)}{d(\theta)} \cdot \frac{1}{\sin \theta} \quad (\text{III-8})$$

A plot of this calculated FFP distribution is shown in Figure III.6.

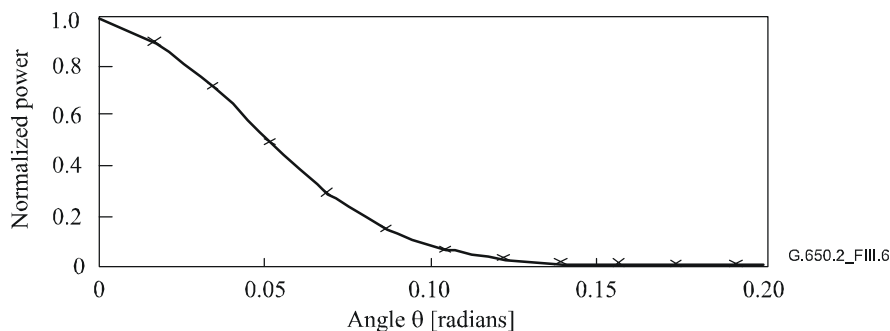


Figure III.6/G.650.2 – Plot of FFP distribution

From the far-field power distribution $F^2(\theta)$, it is then possible to calculate the near-field power distribution $I(r)$ as a function of radius r , using the inverse Hankel transform as follows:

$$I(r) = \left[\int_0^{\infty} \sqrt{F^2(\theta)} \cdot J_0\left(\frac{2\pi r}{\lambda}\right) \sin 2\theta d\theta \right]^2 \quad (\text{III-9})$$

A plot of this calculated near-field distribution $I(r)$ as a function of radius r is shown in Figure III.7.

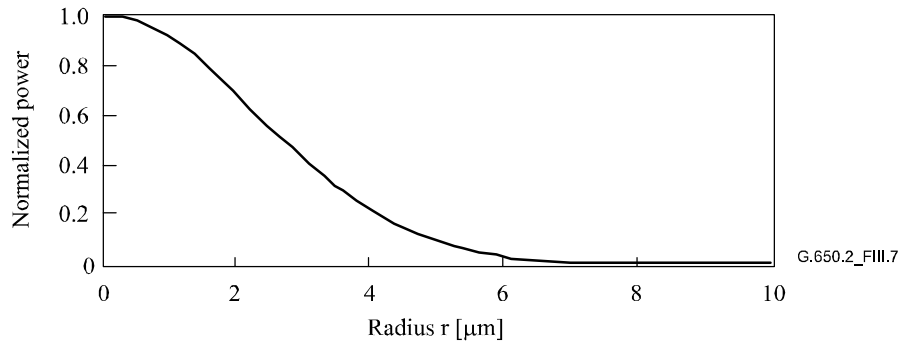


Figure III.7/G.650.2 – Plot of NFP distribution

Effective area, A_{eff} is then calculated from the near-field distribution $I(r)$ using Equation III-10.

$$A_{eff} = 2\pi \cdot \frac{\left[\int_0^{\infty} I(r) \cdot r dr \right]^2}{\int_0^{\infty} I(r)^2 \cdot r dr} \quad (\text{III-10})$$

III.2.4 Presentation of the results

The following details shall be presented:

- a) Test set-up arrangement, dynamic range of the measurement system, processing algorithms, and a description of the aperture assembly used (including the NA).
- b) Launching conditions.
- c) Wavelength and spectral linewidth FWHM of the source.
- d) Fibre identification and length.
- e) Type of cladding mode stripper.
- f) Type and dimensions of the detector.
- g) Temperature of the sample and environmental conditions (when necessary).
- h) Indication of the accuracy and repeatability.
- i) Effective area (A_{eff}).
- j) Plot of $A_{eff}(\lambda)$ (if required).

III.3 The near-field scan (NFS) technique

III.3.1 General

The effective area (A_{eff}) of single mode fibres is determined by the near-field scan (NFS) measurement technique.

III.3.2 Test apparatus

III.3.2.1 Light source (as in 5.1.1.2.1/G.650.1)

III.3.2.2 Modulation (as in 5.1.1.2.2/G.650.1)

III.3.2.3 Launching conditions (as in 5.1.1.2.3/G.650.1)

III.3.2.4 Cladding mode stripper (as in 5.1.1.2.4/G.650.1)

III.3.2.5 Specimen (as in 5.1.1.2.5/G.650.1)

III.3.2.6 Scan apparatus (as in 5.1.1.2.6/G.650.1)

III.3.2.7 Detector (as in 5.1.1.2.7/G.650.1)

III.3.2.8 Amplifier (as in 5.1.1.2.8/G.650.1)

III.3.2.9 Data acquisition (as in 5.1.1.2.9/G.650.1)

III.3.3 Measurement procedure

The launch end of the fibre shall be aligned with the launch beam, and the output end of the fibre shall be aligned to the appropriate output device.

The effective area (A_{eff}) is computed from Equations III-11 to III-15.

III.3.3.1 Equipment calibration

For equipment calibration the magnification of the magnifying optics shall be measured by scanning the length of a specimen whose dimension are already known with suitable accuracy. This magnification shall be recorded.

III.3.3.2 Calculations

III.3.3.2.1 Equations and figures for effective area (A_{eff}) calculation

1) *Calculate the centroid*

For a given cross-section of the near-field pattern (NFP) that is of maximum extent, with position values given by r and intensity values as $I(r_i)$, the centroid position, r_c , is given as:

$$r_c = \frac{\sum r_i I(r_j)}{\sum I(r_i)} \quad (\text{III-11})$$

2) *Fold the intensity profile*

Re-index the position and intensity data around the position r_c so that positions above have index values greater than zero and positions below have index values less than zero. The maximum index is given as n . The folded intensity profile is:

$$I_f(r_i) = \{I(r_i) + I(r_{-i})\} / 2 \quad (\text{III-12})$$

3) *Compute the integrals from Equation III-12*

Use an appropriate numerical integration method to compute the integrals of Equation III-12. The following is an example. Any other integration method shall be at least as accurate.

$$T = \left[\sum_0^m I(r_j) r_j \Delta r \right]^2 \quad (\text{III-13})$$

$$B = \sum_0^m I^2(r_j) r_j \Delta r \quad (\text{III-14})$$

where $\Delta r = r_1 - r_0$

4) *Complete the calculation*

$$A_{eff} = \frac{2\pi T}{B} \quad (\text{III-15})$$

An example of calculated near-field pattern (NFP) is shown in Figure III.7.

III.3.4 Presentation of the results

The following details shall be presented:

- a) Test set-up arrangement, dynamic range of the measurement system, processing algorithms, and a description of the aperture assembly used (including the NA).
- b) Launching conditions.
- c) Wavelength and spectral linewidth FWHM of the source.
- d) Fibre identification and length.
- e) Type of cladding mode stripper.
- f) Type and dimensions of the detector.
- g) Temperature of the sample and environmental conditions (when necessary).
- h) Indication of the accuracy and repeatability.
- i) Effective area (A_{eff}).
- j) Plot of $A_{eff}(\lambda)$ (if required).

Appendix IV

Information on polarization mode dispersion statistics

This appendix is provided to summarize some of the statistical calculations for PMD. IEC 61282-3 documents the calculations and theory more completely. This will be given in the following clauses:

- Introduction.
- Data collection.
- Calculation of PMD_Q (Monte Carlo).
- Calculation for DGD_{max} (Monte Carlo).

NOTE – Other calculation methods are allowed and defined in IEC 61282-3. The Monte Carlo method is given here because it is the easiest to describe.

IV.1 Introduction

Polarization mode dispersion (PMD) is a statistical attribute that, for a given fibre, is defined as the average of measured differential group delay (DGD) values across a range of wavelengths. Since the DGD values are random across time and wavelength, there is a theoretical lower limit to achievable reproducibility of the reported PMD value of approximately $\pm 15\%$. This feature implies that it is not appropriate to select individual fibres or cables to a specification that is tighter than the capability of the process. Such selections are often appropriate for deterministic attributes like attenuation but are not generally appropriate for PMD. This means that a specification on the overall process distribution is most reasonable.

A second consideration regarding the functionality of PMD is that system impairment at a given time and wavelength is controlled by the DGD value, which varies statistically around the PMD value. If the PMD value for a particular cabled fibre is given, the probability that DGD exceeds a given value can be calculated. It is clear, however, that application of these formulae to a maximum specified value will yield a very inaccurate view of the actual system performance. A statistical specification on PMD, however, can lead to a statistical boundary on the DGD values for the population as a whole. This boundary, defined in terms of probability, leads to a value for use in

system design that is approximately 20% lower in DGD value and two orders of magnitude less in probability than the values that would be obtained without a statistical specification.

From the first consideration, it is desirable to define a single statistical metric for the distribution of the PMD values that are measured on optical fibre cables. The metric, therefore, must incorporate both aspects of process mean and process variability. An upper confidence limit at some probability level is such a metric.

It is known that the PMD coefficient of a set of concatenated cables can be estimated by the computation of the quadrature average of the PMD coefficients of the individual cables. To give the upper confidence limit metric more meaning in terms of application, the upper bound for a concatenated link of twenty cables is computed. This number of cable sections is smaller than that used in most links, but is large enough to be meaningful in terms of projecting DGD distributions for concatenated links. A probability value of 0.01% is also standardized, partially on the basis of obtaining equivalence with the probability that DGD exceeds a bound, which is required to be very low. The upper confidence limit is named PMD_Q , or link design value and this specification type is known as Method 1.

The probability limit for DGD is set at $6.5 \cdot 10^{-8}$ based on various system considerations including the presence of other PMD-generating components that may be in the links. IEC 61282-3 describes a method of determining a maximum (defined in terms of probability) so that if a distribution passes the Method 1 requirement, the DGD across links comprised of only optical fibre cable will exceed the maximum DGD with a probability less than $6.5 \cdot 10^{-8}$. The DGD_{\max} value is established for a broad range of distribution shapes. This DGD_{\max} method of specifying the PMD distribution of optical fibre cables is known as Method 2. Methods of combining the Method 2 parameters with those of other optical components are given in IEC 61282-3.

Method 1 is a metric that is based on what is measured and is, therefore, somewhat more straightforward for use in trade and commerce as a normative requirement. Method 2 is a means of extrapolating the implications for system design and is, therefore, included as information for system design.

IV.2 Data collection

The calculations are done with PMD values that are representative of a given cable construction and manufacturing time period. Typically at least 100 values are required. The sample is normally taken on different production cables and different fibre locations within the cables.

The cable distribution can be augmented by measurements of uncabled fibre provided that a stable relationship between uncabled fibre and cable values has been demonstrated for a given construction. One means of such augmentation is to generate several possible cable values from the value of each uncabled fibre. These different values should be selected randomly to represent both the usual relationship and the variability that follows from, for example, measurement reproducibility. Because the range of variations includes reproducibility error, this method of estimating the distribution of cable PMD values can lead to over-estimation of PMD_Q .

The length of the samples measured could seem to have implications on the Method 2 deductions. This has been studied with the following conclusions. The Method 2 implications remain valid for any link less than 400 km as long as either:

- the installed cable sections are less than 10 km; or
- the measured lengths are less than 10 km.

IV.3 Calculation of PMD_Q (Monte Carlo)

Other methods of calculation are given in IEC 61282-3. The Monte Carlo method is described here because it is the easiest to describe and uses the fewest assumptions.

The measured PMD coefficient values are represented by x_i , with i ranging from 1 to N , the number of measurements. These values will be used to generate 100,000 concatenated link PMD coefficient values, each computed with the quadrature average of 20 individual cable values that are randomly selected from the sample population.

NOTE – When $N = 100$, there are $5.3 \cdot 10^{20}$ possible link values.

For each link value computation, select 20 random numbers between 1 and N . Select these values and note them with index, k . The link PMD coefficient, y , is calculated as:

$$y = \left(\frac{1}{20} \sum_{k=1}^{20} x_k^2 \right)^{1/2} \quad (\text{IV-1})$$

Collect the 100,000 values of y into a high density histogram as they are being computed. When this computation is complete, calculate the cumulative probability function from the histogram and determine the PMD value associated with the 99.99% level. Report this value as PMD_Q . If the computed PMD_Q is less than the specified value (0.5 ps/sqrt(km)), the distribution passes Method 1.

IV.4 Calculation for DGD_{\max} (Monte Carlo)

This calculation builds on that of the calculation for PMD_Q . In this calculation, a value of DGD_{\max} is predefined (at 25 ps) and a probability of exceeding this value, P_F , is calculated. If the computed probability is less than the specified value ($6.5 \cdot 10^{-8}$), the distribution passes Method 2.

Before beginning the Monte Carlo, calculate the PMD coefficient limit, P_{\max} , as:

$$P_{\max} = \frac{\text{DGD}_{\max}}{\sqrt{L_{\text{ref}}}} = \frac{25}{20} = 1.25$$

For each subsequent pair of 20 cable link concatenation values, y_j and y_{j+1} , a 40-cable concatenation value, z_j , is generated as:

$$z_j = \left(\frac{y_j^2 + y_{j+1}^2}{2} \right)^{1/2} \quad (\text{IV-2})$$

NOTE – This yields 50,000 values of z_j , an adequate number.

Calculate the probability of exceeding DGD_{\max} on the j th concatenation of 40 links, p_j , as:

$$p_j = 1 - \int_0^{P_{\max}/z_j} 2 \left(\frac{4}{\pi} \right)^{3/2} \frac{t^2}{\Gamma(3/2)} \exp \left[-\frac{4}{\pi} t^2 \right] dt \quad (\text{IV-3})$$

Excel™ defines a function that can compute p_j , $\text{GAMMADIST}(X, \text{ALPHA}, \text{BETA}, \text{Cumulative})$. The call to this function should be:

$$PJ = 1 - \text{GAMMADIST}(4 \times P_{\max} \times P_{\max} / (\pi) \times ZI \times ZI, 1.5, 1, \text{TRUE}) \quad (\text{IV-4})$$

The probability of exceeding DGD_{\max} , P_F , is given as:

$$P_F = \frac{1}{50000} \sum_j p_j \quad (\text{IV-5})$$

If P_F is less than the specified value, the distribution passes Method 2.

SERIES OF ITU-T RECOMMENDATIONS

Series A	Organization of the work of ITU-T
Series D	General tariff principles
Series E	Overall network operation, telephone service, service operation and human factors
Series F	Non-telephone telecommunication services
Series G	Transmission systems and media, digital systems and networks
Series H	Audiovisual and multimedia systems
Series I	Integrated services digital network
Series J	Cable networks and transmission of television, sound programme and other multimedia signals
Series K	Protection against interference
Series L	Construction, installation and protection of cables and other elements of outside plant
Series M	Telecommunication management, including TMN and network maintenance
Series N	Maintenance: international sound programme and television transmission circuits
Series O	Specifications of measuring equipment
Series P	Telephone transmission quality, telephone installations, local line networks
Series Q	Switching and signalling
Series R	Telegraph transmission
Series S	Telegraph services terminal equipment
Series T	Terminals for telematic services
Series U	Telegraph switching
Series V	Data communication over the telephone network
Series X	Data networks, open system communications and security
Series Y	Global information infrastructure, Internet protocol aspects and next-generation networks
Series Z	Languages and general software aspects for telecommunication systems